showed that repeated injection of the rat Epo gene lost its efficacy of expression of protein in the serum in rats, and the mechanism remains unclear [34]. In addition to the duration of elevated serum HGF level, Arthur *et al.* reported that there is a plateau above which a further increase in HGF levels provides no added benefit in HLA-B27 transgenic rats treated with recombinant HGF [21]. Recently, Mukoyama *et al.* reported the therapeutic effect of adenoviral-mediated HGF gene administration via the intrarectal route on TNBS-induced colitis [39]. The method could transfect the gene successfully into the epithelial cells of the colon without elevation of serum HGF levels. This could avoid the side effect of overly expressed serum HGF in serum on organs other than the intestine. On the contrary, the direct transfection of the gene into epithelial cells carries the risk of carcinogenesis of the colon [35], especially considering the chronic intestinal inflammatory status of patients with inflammatory bowel disease. We must be cautious when choosing the best method for HGF gene transfer, to enable HGF to work maximally in the target organ of the intestine.

In conclusion, this study demonstrated that hydrodynamics-based transfection of the rat HGF gene into the liver via tail vein injection ameliorated DSS colitis in mice, and its effect appears to depend on the duration of elevated serum HGF level. These results suggest that HGF gene therapy could be a new therapeutic approach to inflammatory bowel disease.

Acknowledgements

We thank Norio Honda and Takao Tsuchida for technical assistance and Dr. Minoru Nomoto, Dr. Terasu Honma, and Dr. Yasunobu Matsuda for helpful discussions. We also thank Dr. Suresh S. Palaniyandi for editing the English in the manuscript. This work was supported by grants from the Ministry of Health, Welfare, and Labor of the Government of Japan.

References

1. Podolsky DK. Inflammatory bowel disease. *N Engl J Med* 2002; **347**: 417–429.
2. Sands BE. Therapy of inflammatory bowel disease. *Gastroenterology* 2000; **118**: S68–S82.
3. Shanahan F. Inflammatory bowel disease: immunodiagnostics, immunotherapeutics, and ecotherapeutics. *Gastroenterology* 2001; **120**: 622–635.
4. Sandborn WJ, Targan SR. Biologic therapy of inflammatory bowel disease. *Gastroenterology* 2002; **122**: 1592–1608.
5. Targan SR, Hanauer Sb, van Deventer SJ, *et al.* A short-term study of chimeric monoclonal antibody cA2 to tumor necrosis factor alpha for Crohn's disease. Crohn's Disease cA2 Study Group. *N Engl J Med* 1997; **337**: 1029–1035.
6. Ito H, Takazoe M, Fukuda Y, *et al.* A pilot randomized trial of a human anti-interleukin-6 receptor monoclonal antibody in active Crohn's disease. *Gastroenterology* 2004; **126**: 989–996.
7. Playford RJ. Peptides and gastrointestinal mucosal integrity. *Gut* 1995; **37**: 595–597.
8. Procaccino F, Reinshagen M, Hoffmann P, *et al.* Protective effect of epidermal growth factor in an experimental model of colitis in rats. *Gastroenterology* 1994; **107**: 12–17.
9. Sinha A, Nightingale JMD, West KP, *et al.* Epidermal growth factor enemas with oral mesalamine for mild-to-moderate left-sided ulcerative colitis. *N Engl J Med* 2003; **349**: 350–357.
10. Boros P, Miller CM. Hepatocyte growth factor: a multifunctional cytokine. *Lancet* 1995; **345**: 293–295.
11. Zarnegar R, Michalopoulos GK. The many faces of hepatocyte growth factor: from heptopoiesis to hematopoiesis. *J Cell Biol* 1995; **129**: 1177–1180.
12. Nakamura T, Nishizawa T, Hagiya M, *et al.* Molecular cloning and expression of human hepatocyte growth factor. *Nature* 1989; **342**: 440–443.
13. Nishimura S, Takahashi M, Ota S, *et al.* Hepatocyte growth factor accelerates restitution of intestinal epithelial cells. *J Gastroenerol* 1998; **33**: 172–178.
14. Tsuji S, Kawano S, Tsujii M, *et al.* Roles of hepatocyte growth factor and its receptor in gastric mucosa. A cell biological and molecular biological study. *Dig Dis Sci* 1995; **40**: 1132–1139.
15. Nusrat A, Parkos CA, Bacarra AE, *et al.* Hepatocyte growth factor/scatter factor effects on epithelia. Regulation of intercellular junctions in transformed and nontransformed cell lines, basolateral polarization of c-met receptor in transformed and natural intestinal epithelia, and induction of rapid wound repair in a transformed model epithelium. *J Clin Invest* 1994; **93**: 2056–2065.
16. Bottaro DP, Rubin JS, Faletto DL, *et al.* Identification of the hepatocyte growth factor receptor as the c-met proto-oncogene product. *Science* 1991; **251**: 802–804.
17. Itoh H, Naganuma S, Takeda N, *et al.* Regeneration of injured intestinal mucosa is impaired in hepatocyte growth factor activator-deficient mice. *Gastroenterology* 2004; **127**: 1423–1435.
18. Kitamura S, Kondo S, Shinomura Y, *et al.* Expression of heptocyte growth factor and c-met in ulcerative colitis. *Inflamm Res* 2000; **49**: 320–324.
19. Ortega-Cava CF, Ishihara S, Kawashima K, *et al.* Hepatocyte growth factor expression in dextran sodium sulfate-induced colitis in rats. *Dig Dis Sci* 2002; **47**: 2275–2285.
20. Tahara Y, Ido A, Yamamoto S, *et al.* Hepatocyte growth factor facilitates colonic mucosal repair in experimental ulcerative colitis in rats. *J Pharmacol Exp Ther* 2003; **307**: 146–151.
21. Arthur G, Schwartz MZ, Kuenzler KA, Birbe R. Hepatocyte growth factor treatment ameliorates diarrhea and bowel inflammation in a rat model of inflammatory bowel disease. *J Pediatr Surg* 2004; **39**: 139–143.
22. Hickman MA, Malone RW, Lehmann-Bruinsma K, *et al.* Gene expression following direct injection of DNA into liver. *Hum Gene Ther* 1994; **5**: 1477–1483.
23. Paillard F. Naked DNA gene delivery to the liver. *Hum Gene Ther* 1997; **8**: 1735–1736.
24. Liu F, Song Y, Liu D. Hydrodynamics-based transfection in animals by systemic administration of plasmid DNA. *Gene Ther* 1999; **6**: 1258–1266.
25. Sasaki S, Yoneyama H, Suzuki K, *et al.* Blockade of CXCL10 protects mice from acute colitis and enhances crypt cell survival. *Eur J Immunol* 2002; **32**: 3197–3205.
26. M Noguchi, N Hiwatashi, Z Liu, T Toyota. Secretion imbalance between tumor necrosis factor and its inhibitor in inflammatory bowel disease. *Gut* 1998; **43**: 203–209.
27. Hacein-Bey-Abina S, von Kalle C, Schmidt M, *et al.* A serious adverse event after successful gene therapy for X-linked severe combined immunodeficiency. *N Engl J Med* 2003; **348**: 255–256.
28. Hacein-Bey-Abina S, Von Kalle C, Schmidt M, *et al.* LMO2-associated clonal T cell proliferations in two patients after gene therapy for SCID-X1. *Science* 2003; **302**: 415–419.
29. Ueki T, Kaneda Y, Tsutsui H, *et al.* Hepatocyte growth factor gene therapy of liver cirrhosis in rats. *Nat Med* 1999; **5**: 226–230.
30. Kuroiwa T, Kakishita E, Hamano T, *et al.* Hepatocyte growth factor ameliorates acute graft-versus-host disease and promotes hematopoietic function. *J Clin Invest* 2001; **107**: 1365–1373.
31. Zhang G, Budker V, Wolff JA. High levels of foreign gene expression in hepatocytes after tail vein injections of naked plasmid DNA. *Hum Gene Ther* 1999; **10**: 1735–1737.
32. Zhang G, Song YK, Liu D. Long-term expression of human alpha1-antitrypsin gene in mouse liver achieved by intravenous administration of plasmid DNA using a hydrodynamics-based procedure. *Gene Ther* 2000; **7**: 1344–1349.
33. Miao CH, Thompson AR, Loeb K, *et al.* Long-term and therapeutic-level hepatic gene expression of human factor IX after naked plasmid transfer in vivo. *Mol Ther* 2001; **3**: 947–957.

34. Maruyama H, Higuchi N, Nishikawa Y, *et al.* High-level expression of naked DNA delivered to rat liver via tail vein injection. *J Gene Med* 2002; **4**: 333–341.
35. Takayama H, LaRochelle WJ, Sharp R, *et al.* Diverse tumorigenesis associated with aberrant development in mice overexpressing hepatocyte growth factor/scatter factor. *Proc Natl Acad Sci U S A* 1997; **94**: 701–706.
36. Oh K, Iimuro Y, Takeuchi M, *et al.* Ameliorating effect of hepatocyte growth factor on inflammatory bowel disease in a murine model. *Am J Physiol* 2004; **288**: 729–735.
37. Okayasu I, Hatakeyama S, Ohkusa T, Inagaki Y, Nakaya R. A novel method in the induction of reliable experimental acute and chronic ulcerative colitis in mice. *Gastroenterology* 1990; **98**: 694–702.
38. Cooper HS, Murthy SN, Shah RS, Sedergran DJ. Clinicopathologic study of dextran sulfate sodium experimental murine colitis. *Lab Invest* 1993; **69**: 238–249.
39. Mukoyama T, Kanbe T, Murai R, *et al.* Therapeutic effect of adenoviral-mediated hepatocyte growth factor gene administration on TNBS-induced colitis in mice. *Biochem Biophys Res Commun* 2005; **329**: 1217–1224.

ELSEVIER

Journal of Hepatology 45 (2006) 254–262

Journal of Hepatology

www.elsevier.com/locate/jhep

Increase of CD4 $^{+}$ CD25 $^{+}$ regulatory T-cells in the liver of patients with hepatocellular carcinoma

Xiu Hua Yang[1,†], Satoshi Yamagiwa[1], Takafumi Ichida[2,*], Yasunobu Matsuda[1], Satoshi Sugahara[1], Hisami Watanabe[3], Yoshinobu Sato[4], Toru Abo[5], David A. Horwitz[6], Yutaka Aoyagi[1]

[1]*Division of Gastroenterology and Hepatology, Niigata University Graduate School of Medical and Dental Sciences, Niigata, Japan*
[2]*Division of Gastroenterology and Hepatology, Juntendo University School of Medicine, 2-1-1 Hongo, Bunkyo-ku, Tokyo 113-8421, Japan*
[3]*Division of Cellular and Molecular Immunology, Center of Molecular Bioscience, University of the Ryukyu, Okinawa, Japan*
[4]*Division of Surgery, Niigata University Graduate School of Medical and Dental Sciences, Niigata, Japan*
[5]*Division of Immunology, Niigata University Graduate School of Medical and Dental Sciences, Niigata, Japan*
[6]*Division of Rheumatology and Immunology, Department of Internal Medicine, Keck School of Medicine, University of Southern California, Los Angeles, CA, USA*

See Editorial, pages 178–181

***Background/Aims*: The immune response to tumor-specific antigens is typically unable to control the growth and spread of malignant cells. Accumulating evidence indicates that the suppressive effects of CD4 $^{+}$ CD25 $^{+}$ regulatory T-cells are at least partially responsible for the failure of immune-mediated elimination of tumor cells.**

***Methods*: We have studied 25 patients with hepatocellular carcinoma (HCC). The liver tissues with HCC were separated into the marginal region of tumor (peri-tumor region) and the non-tumor region distant from the tumor. CD4 $^{+}$ CD25 $^{+}$ T-cells were quantified in the blood and the liver by flow cytometry and immunohistochemistry, and their effect on T-cell proliferation and activation was determined.**

***Results*: We found a significant increase in both the proportion and absolute numbers of CD4 $^{+}$ CD25 $^{+}$ T-cells in the peri-tumor regions, but not in unaffected areas (9.5 ± 4.5 vs. 4.6 ± 2.8%, $P = 0.011$). CD4 $^{+}$ CD25 $^{+}$ T-cells isolated from peri-tumor regions displayed phenotype markers characteristic of regulatory T-cells, and expressed Foxp3 mRNA. CD8 $^{+}$ T-cells in peri-tumor regions were inversely proportional to CD4 $^{+}$ CD25 $^{+}$ T-cells in the same region ($P < 0.001$). Moreover, isolated CD4 $^{+}$ CD25 $^{+}$ T-cells inhibited autologous CD8 $^{+}$ T-cell proliferation.**

***Conclusions*: Our results suggest that CD4 $^{+}$ CD25 $^{+}$ T-cells in the marginal region of HCC may play a critical role in controlling CD8 $^{+}$ cytotoxic T-cell activity and, thereby, contribute to the progression of HCC.**

Keywords: **Regulatory T-cells; Tumor immunity; Hepatocellular carcinoma; Intrahepatic lymphocytes; Cytotoxic T lymphocytes**

Received 30 January 2005; received in revised form 14 January 2006; accepted 25 January 2006; available online 9 March 2006

* Corresponding author. Tel.: + 81 55 948 3111; fax: + 81 55 948 5088.
E-mail address: takafumi@med.juntendo.ac.jp (T. Ichida).

Abbreviations: Ab, antibody; CH, chronic hepatitis; CTL, cytotoxic T lymphocytes; FITC, fluorescein isothiocyanate; HBV, hepatitis B virus; HCC, hepatocellular carcinoma; HCV, hepatitis C virus; mAb, monoclonal antibody; MNCs, mononuclear cells; PBL, peripheral blood lymphocytes; LC, liver cirrhosis; LDLT, living donor liver transplantation.

† Present address: General Surgery Department, The First Hospital Affiliated Harbin medical University, Harbin, China.

1. Introduction

The response of T-cells to self and non-self antigens is controlled by a network of regulatory T (Treg) cells. Many subsets of Treg cells have been described and recently much progress has been made in understanding their ontogeny, function, and mechanism of action [1–3]. CD4 $^{+}$ cells that constitutively express CD25, the interleukin-2-receptor α-chain, are generally

0168-8278/$32.00
doi:10.1016/j.jhep.2006.01.036

considered to be natural Treg cells, and constitute 5–10% of peripheral $CD4^+$ T-cells in healthy animals and humans [4–6]. These cells are partially anergic, but require activation via their T-cell receptors to become suppressive and to inhibit the proliferation of other T-cells [7–9]. We have shown that naïve human $CD4^+$ cells activated with allogeneic stimulator cells in the presence of TGF-β become potent $CD25^+$ suppressor cells with a phenotype and functional properties similar, if not identical, with natural $CD4^+CD25^+$ Treg cells [10].

Although, it is well recognized that many tumors bear antigens that can induce T-cell cytotoxic responses, tumor immunity is generally weak and unable to prevent tumor growth [11]. As many tumor-associated antigens recognized by autologous T-cells in cancer patients have now turned out to be normal self-constituents, tumor immunity should be considered as in part autoimmunity [12]. It has become apparent that $CD4^+CD25^+$ T-cells phenotypically similar to natural Treg cells block effective tumor immunity. It has been reported that elimination or reduction of $CD4^+CD25^+$ T-cells can induce effective tumor immunity in otherwise non-responding mice by activating tumor-specific cytotoxic T lymphocytes [13,14]. The beneficial effect on tumor immunity associated with the removal of $CD4^+CD25^+$ Treg cells suggests that these cells play a critical role in immunologic tolerance of tumor cells.

Although, several groups have reported increased number of $CD4^+CD25^+$ Treg cells in the peripheral blood (PB) of cancer patients [15–17], there are only a few studies that described an increase of $CD4^+CD25^+$ Treg cells in tumor-infiltrating lymphocytes (TILs) or tumor-associated lymphocytes [18–20]. One group has reported that $CD4^+CD25^+$ T-cells are increased in the TILs of patients with lung cancer. $CD4^+CD25^+$ T-cells isolated from these tumors strongly inhibited the proliferation of autologous PB T-cells stimulated by anti-CD3/CD28 [19].

In patients with hepatocellular carcinoma (HCC), one group has quantified $CD4^+CD25^+$ Treg cells in the PB of these patients [17], but information on the numbers of these cells in the liver is not available. The adult human liver contains large numbers of lymphocytes with a unique phenotypic distribution compared with the PB and other organs, and has distinctive features in the immune system [21–23]. The principal objective of the current study was to investigate the numbers of $CD4^+CD25^+$ T-cells in tumor-involved and non-involved areas of the liver of patients with HCC. We have observed large numbers of $CD4^+CD25^+$ T-cells in the marginal region of HCC, and have evidence suggesting that these cells may be involved in the suppression of tumor immunity against HCC.

2. Patients and methods

2.1. Patients

After obtaining appropriate informed consent in writing under institutional review board-approved protocols, blood and surgically removed liver tissues, or liver biopsy specimens were collected from patients with HCC, chronic hepatitis (CH) or liver cirrhosis (LC) without HCC, and normal donors for living donor liver transplantation. Information regarding patient profiles and tumor stage of HCC patients was shown in Table 1. Twenty-five patients (9 female, 16 male) with HCC were investigated. Mean age was 61.8 ± 11.2 years (range, 39–76 years). Twelve patients were diagnosed as CH, and 13 patients as LC by histological examination. The mean age of 38 patients (11 female, 27 male) with CH or LC without HCC was 60.4 ± 11.7 years (range, 35–72 years). Seven patients were positive for HBV, and 31 patients for HCV. Thirty patients were diagnosed as CH, and 8 patients as LC by histological examination. The mean age of 15 normal donors (6 female, 9 male) was 34.3 ± 12.6 years (range, 20–59 years). The donors did not have any history of liver disease.

2.2. Reagents

Antibodies used were anti-CD3 (UCHT1); anti-CD4 (RPA-T4); anti-CD8 (RPA-T8); anti-CD25 (M-A251); anti-CD45RA (HI100); anti-CD45RO (UCHL-1); anti-CD69 (FN50); anti-CD152 (cytotoxic T-lymphocyte-associated antigen-4; CTLA-4) (BNI3) (PharMingen, San Diego, CA); anti-glucocorticoid-induced TNFR-related gene (GITR) (110416, R&D Systems, Inc., Minneapolis, MN). Anti-CD4 (MT310) and anti-CD25 (ACT-1) antibodies for immunohistochemistry were purchased from DAKO (Glostrup, Denmark).

2.3. Cell isolation

The removed liver tissues with HCC were separated into two parts, the marginal region of tumor (peri-tumor region) and the non-tumor region that was more than 5 cm distant from the tumor margin (non-tumor region). The specimens from peri-tumor regions contained part of the tumor. The tissues were pressed through stainless steel mesh and suspended in Eagle's MEM medium (Life Technologies, Grand Island, NY) supplemented with 5 mM HEPES and 5% heat-inactivat-

Table 1
Characteristics of the 25 patients with HCC

Variable	Results
Mean age (year) (mean±SD)	61.8 ± 11.2
Gender (male/female)	16/9
Virus: HBV/HCV	7/18
Background: CH/LC	12/13
Child-Pugh classification (A/B/C)	18/5/2
Tumor factors	
Tumor size (cm)[a] (≤ 3.0/ > 3.0)	15/10
Number of tumors (Single/double/multiple)	14/6/5
Stage[b] (I/II/III/IV)	0/14/6/5
Histology (well/moderately/poorly)[a]	6/12/7
Cases with histological vascular invasion	28% (7/25)
Cases with histological metastatic foci	24% (6/25)
Operation	
Partial/segmentectomy/lobectomy/LDLT	9/6/5/5

HBV, hepatitis B virus; HCV, hepatitis C virus; CH, chronic hepatitis; LC, liver cirrhosis; HCC, well, well-differentiated; HCC, moderately, moderately differentiated; HCC, poorly, poorly differentiated; HCC, partial, partial resection; LDLT, living-donor liver transplantation.

[a] In case of multiple tumors, tumor size and histology are expressed by examining the largest tumor.

[b] According to the Japanese general rules for primary liver cancer.

ed FCS. Heparinized peripheral blood was obtained at the time of tumor collection. Mononuclear cells (MNCs) were separated by Ficoll-Paque (Pharmacia, Piscataway, NJ) density gradient centrifugation. $CD3^+$ and $CD4^+$ cells were purified from MNCs obtained from blood and peri-tumor regions of HCC, respectively, by isolation with immunomagnetic beads (Miltenyl Biotech, Auburn, CA). In the case of isolated $CD4^+$ cells, anti-CD4 beads were detached and stained with anti-CD25 beads (Miltenyl Biotech), followed by positive and negative selection (purity of $CD4^+CD25^+$ population: > 95%; $CD4^+CD25^-$ population: > 95%, $CD3^+$ population: > 98%).

2.4. Flow-cytometry

Cell surface antigen expression was determined by a three-color immunofluorescence assay. Cells (10^5) were incubated with the appropriate FITC-, phycoerythrin- or CyChrome-conjugated Abs for 30 min. at 4 °C in PBS with 0.1% FCS and 0.02 mM NaN_3. Cytoplasmic CTLA-4 was determined by intracellular staining as described previously [10]. To analyze cell divisions, labeling of purified $CD3^+$ T-cells with 5-(and 6-) carboxyfluorescein diacetate succinimidyl ester (CFSE; Molecular Probes, Inc., Eugene, OR) was performed as described previously [10]. After wash, the labeled cell samples were analyzed on FACScan (Becton Dickinson, San Jose, CA).

2.5. Immunohistochemistry

Cryostat sections 5-μm thick were cut and fixed in cold acetone for 5 min. After immersion in blocking serum, sections were incubated with mouse anti-human CD25 or CD4 mAb (DAKO) at a 1:50 or 1:100 dilution, respectively, in PBS supplemented with 3% BSA at 4 °C overnight. After successive washing in PBS, sections were incubated with biotinylated anti-mouse immunoglobulin at a 1:100 dilution in PBS supplemented 5% BSA.

Immunohistochemical detection was performed according to the avidin–biotin-peroxidase complex method using the Vectastain Elite ABC kit (Vector Laboratories, Inc., Burlingame, CA). Sections were finally developed with diaminobenzidine (DAB) substrate (Muto Pure Chemicals, Tokyo, Japan) or Vector SG (Vector Laboratories). Specimens then were counterstained with Methyl Green solution and mounted.

2.6. Proliferation assay

Ninety-six-well plates were coated with 1 μg/ml anti-CD3 mAb overnight at 4 °C. Purified $CD3^+$ or CFSE-labeled $CD3^+$ cells from patients with HCC were cultured in the plate adding anti-CD28 mAb (1 μg/ml) in RPMI 1640 (Life Technologies) supplemented with 10% FCS at 5×10^4/200 μl per well in triplicate at 37 °C 5% CO_2. Purified $CD4^+CD25^+$ or $CD4^+CD25^-$ cells were added at varying numbers. Blocking experiments were performed with 10 μg/ml anti-TGF-β1 Ab (9016.2, R&D Systems). Purified $CD4^+CD25^+$ and $CD4^+CD25^-$ cells were also cultured in the presence of immobilized anti-CD3 (1 μg/ml) and anti-CD28 mAbs (1 μg/ml) at 5×10^4/200 μl per well in triplicate at 37 °C 5% CO_2. Proliferation was assayed by measuring [^{3}H]thymidine incorporation, and cell division was analyzed by measuring CFSE levels gated on $CD8^+$ cells by flow-cytometry.

2.7. RT-PCR

mRNA content of 5×10^5 viable T-cells was isolated using the RNeasy Protect mRNA extraction kit (Qiagen, Carsbad, CA) following manufacturer's instructions. RT-PCR for Foxp3 and control β-actin mRNA was performed using SuperScript One-Step RT-PCR kit (Invitrogen Corp., Carlsbad, CA) and primers as described previously [24].

2.8. Statistical analysis

The compared *t*-test with Welch's correction or Mann–Whitney *U*-test was used to evaluate the significance of the differences. Correlations between parameters were determined by linear regression analysis. Statistical analysis was performed with GraphPad software, (GraphPad Software, Inc., San Diego, CA). The level of significance was set at $P < 0.05$.

3. Results

3.1. Significant increase of $CD4^+$ $CD25^+$ T-cells in peri-tumor regions of HCC

Analysis of MNCs ($CD45^+$) isolated from patients and controls revealed that the percentage of $CD4^+CD25^+$ T-cells was significantly increased in peri-tumor regions of the liver in patients with HCC in comparison to controls ($P = 0.011$) and patients with CH or LC without HCC ($P = 0.031$) (Fig. 1A). We found a higher proportion of $CD4^+CD25^+$ T-cells in peri-tumor regions of HCC with microvascular invasion (Table 1) than that without invasion, although the difference was not significant (10.7 ± 3.7 vs. $9.5 \pm 4.8\%$, $P = 0.49$). The values of $CD4^+CD25^+$ T-cells in peri-tumor regions of HCC did not correlate with the stages of tumor and the background liver diseases (data not shown). The percentages of $CD3^+$ cells in peri-tumor and non-tumor regions were 67.2 ± 14.4 and $66.7 \pm 13.7\%$, respectively, and the difference was not significant. In contrast, $CD4^+CD25^+$ T-cells in the PB of patients with HCC were significantly decreased in comparison to both controls and patients without HCC ($P = 0.012$ and 0.027, respectively) (Fig. 1B). Representative profiles of CD4/CD25 expression in the liver and PB from a patient with HCC are shown in Fig. 2.

We then determined absolute cell numbers of $CD4^+CD25^+$ T-cells in the liver based on total MNC counts. Total MNCs in the liver with HCC were significantly higher than in the liver of controls ($P = 0.003$) (Table 2). In addition to increased percentages, the total number of $CD4^+CD25^+$ T-cells was significantly higher in peri-tumor regions of HCC than in controls

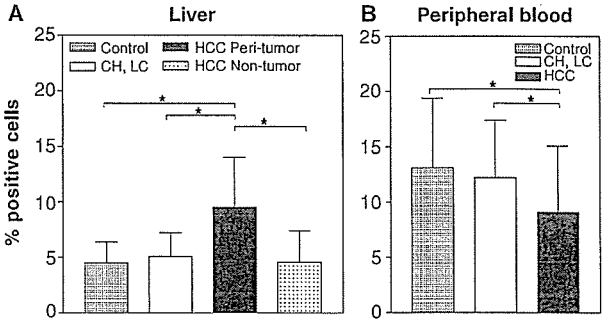

Fig. 1. $CD4^+$ $CD25^+$ T-cells are significantly increased in peri-tumor regions of the liver with HCC. Lymphocytes were obtained from the liver (A) and peripheral blood (B), and stained with CD4, CD25 and CD45. CD45-positive cells were gated and analyzed. The mean + SD are represented. *$P < 0.05$.

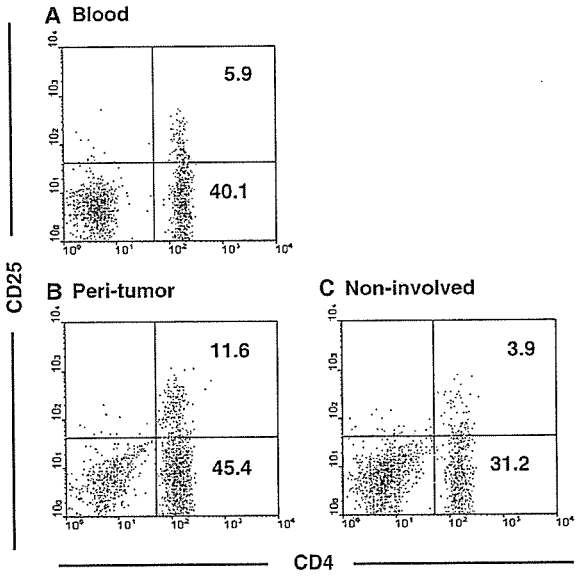

Fig. 2. CD4 + CD25 + T-cells in the liver and the peripheral blood of a patient with HCC. Results of flow cytometric analysis from a representative patient are shown. Lymphocytes were obtained from a 63-year old female patient with HCC (Stage II) + CH (type C). Three-color staining for CD4, CD25 and CD45 was performed, and CD45-positive cells were gated and analyzed. (A) peripheral blood, (B) peri-tumor region of HCC, (C) non-involved region of HCC. Numbers indicate the percentages in the corresponding areas.

($P = 0.001$), patients without HCC ($P = 0.007$), and in non-tumor regions of HCC ($P = 0.004$).

3.2. Phenotypic analysis of CD4 + CD25 + T-cells

Recent studies have shown that CTLA-4 and GITR are up-regulated on CD4 + CD25 + Treg cells [3,4]. Among CD4 + CD25 + T-cells from peri-tumor regions, 70–80% were positive for intracellular CTLA-4 expression, whereas about 50% in the liver of patients with CH without HCC (Fig. 3A). In contrast to the near-uniform expression of CTLA-4 on CD4 + CD25 + T-cells in peri-tumor regions, only 15% of peripheral CD4 + CD25 + T-cells from HCC patients stained positive for CTLA-4 (Fig. 3A). The peripheral CD4 + CD25 + T-cells in patients with CH without HCC showed higher expression of CTLA-4 than those of patients with HCC. Further studies of CD4 + CD25 + T-cells in peri-tumor regions of HCC revealed that they were mostly CD45RA− (Fig. 3B). In the PB more than 50% of CD25− cells were naïve CD45RA + cells, whereas in the liver most of this subset were previously activated CD45RA− cells. Furthermore, we detected an increased expression of GITR on CD4 + CD25 + T-cells from peri-tumor regions of HCC (Fig. 3C). Enhanced expression of CTLA-4 and GITR on peri-tumor CD4 + CD25 + T-cells and decreased expression of CD45RA are consistent with a regulatory phenotype. These studies provide additional evidence that CD4 + CD25 + T-cells from the peri-tumor region of HCC had a regulatory phenotype.

Table 2
Absolute cell numbers of CD4 + CD25 + cells in the liver

Donors	Absolute cell numbers[a]		
	No. of donors	Total MNCs ($\times 10^6$/g liver)	CD4 + CD25 + cells ($\times 10^4$/g liver)
Normal	5	2.4 ± 0.4	7.9 ± 4.9
Liver cirrhosis without HCC	7	3.1 ± 1.4	13.9 ± 4.1†
Hepatocellular carcinoma			
Peri-tumor	10	3.9 ± 0.9*	24.5 ± 8.2*,‡
Non-tumor	10	2.9 ± 2.2	15.5 ± 3.9*

MNCs, mononuclear cells. * Significantly ($P < 0.01$) higher than in control; † significantly ($P < 0.05$) higher than in control; ‡ significantly ($P < 0.01$) higher than in non-tumor regions and LC without HCC.
[a] Mean±standard deviation.

3.3. Immunohistochemical detection of CD4 + CD25 + T-cells in the liver with HCC

The distribution of CD4 + CD25 + T-cells in the liver with immunohistochemistry using serial sections was then examined. Hematoxylin–eosin staining of marginal region of HCC of a patient with LC shows many MNCs infiltrated around the well-differentiated HCC (Fig. 4A). Serial sections revealed CD25 + cells abundant around the tumor, but only a small number of these cells were in the tumor (Fig. 4B). Fig. 4C and D show double staining of CD4 and CD25, and these figures show that almost all the CD25 + cells detected in Fig. 4B are CD4CD25 double-positive cells.

Fig. 5 shows that only a small number of the many infiltrating cells are CD25 + in non-tumor region of the liver of the same patient. These results are consistent with our results determined by flowcytometry.

3.4. Relationship between CD8 + cells and CD4 + CD25 + T-cells in the liver with HCC

CD4 + CD25 + Treg cells have been shown to suppress the generation or activation of CTL [5,10]. To examine the relationship between CD4 + CD25 + T-cells and CD8 + CTL, we plotted percentages of these cells in each case in the liver of patients with HCC in Fig. 6A. In peri-tumor regions, patients with increased CD4 + CD25 + T-cells were associated with smaller numbers of CD8 + cells. Although, there was some variability, the proportion of CD8 + cells was inversely proportional to CD4 + CD25 + T-cells in peri-tumor regions ($r = -0.615$, $P < 0.001$).

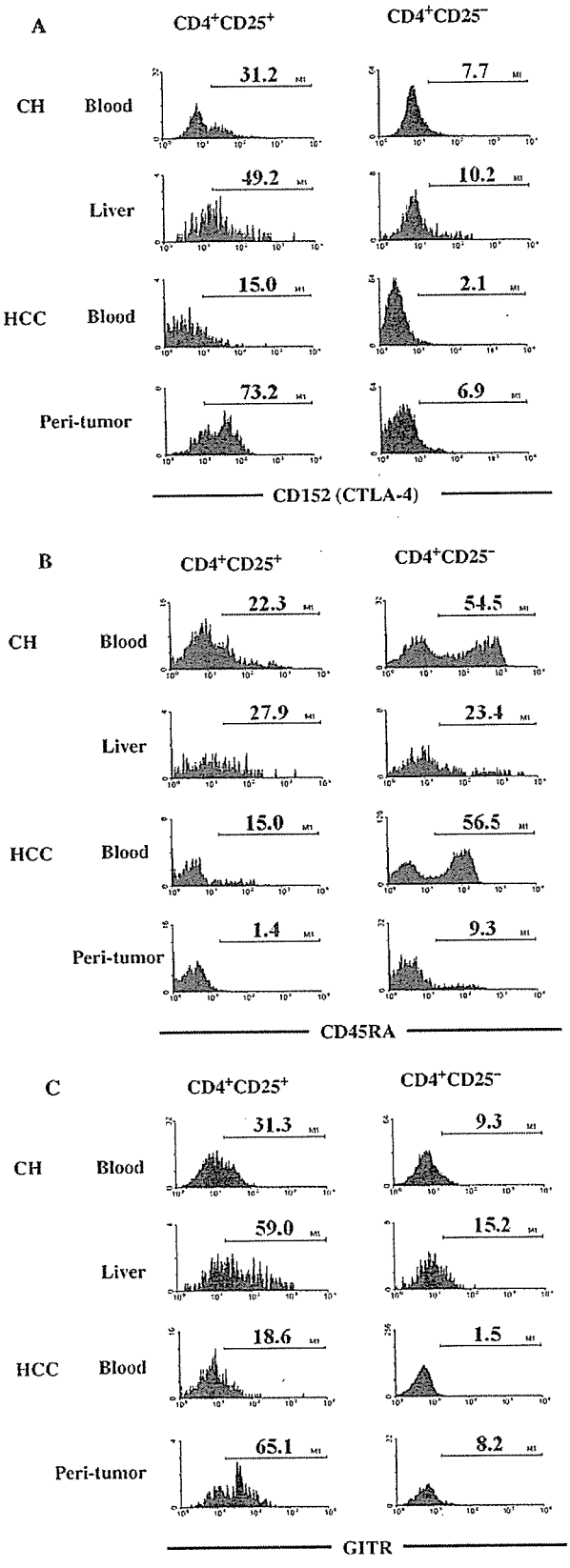

3.5. Suppressive properties of CD4 $^+$ CD25 $^+$ T-cells isolated from the peri-tumor region of HCC

To assess the function of the abundant CD4 $^+$ CD25 $^+$ T-cells found in peri-tumor regions of HCC, we isolated them using immunomagnetic beads and determined their effect on T-cell proliferation and activation. Autologous PB T-cell proliferation was significantly suppressed by addition of CD4 $^+$ CD25 $^+$ T-cells derived from peri-tumor regions of HCC ($P = 0.002$ at 5:1 ratio) (Fig. 7A). The addition of anti-TGF-β1 Ab did not abrogate the suppressive effect (data not shown). CD4 $^+$ CD25 $^+$ T-cells derived from non-tumor regions of HCC patients also suppressed autologous PB T-cell proliferation ($P = 0.008$ at 5:1 ratio) (Fig. 7A). Cell division of CD8 $^+$ cells and the expression of CD69, which is one of early activation markers, on CD8 $^+$ cells were also suppressed by adding CD4 $^+$ CD25 $^+$ T-cells derived from peri-tumor regions of HCC (Fig. 7B, C).

We also examined the proliferation of CD4 $^+$ CD25 $^+$ and CD25 $^+$ CD25 $^-$ T-cells from peri-tumor regions of HCC. CD4 $^+$ CD25 $^+$ T-cells were unresponsive upon stimulation with anti-CD3/CD28 mAbs, relative to CD4 $^+$ CD25 $^-$ T-cells (Fig. 8A). As Foxp3 is now recognized as a master control gene for the development and function of Treg cells [25], we analyzed Foxp3 mRNA expression with RT-PCR. As shown in Fig. 8B, Foxp3 mRNA expression was observed in CD4 $^+$ CD25 $^+$ T-cells isolated from peri-tumor regions of HCC. Together these results suggest that CD4 $^+$ CD25 $^+$ T-cells in peri-tumor regions of HCC had characteristics of Treg cells and might inhibit the activation and proliferation of CD8 $^+$ cells that respond to HCC.

4. Discussion

This study documents increased numbers of CD4 $^+$ CD25 $^+$ T-cells in the peri-tumor region of HCC and provides strong evidence that these are predominantly Treg cells. Isolated CD4 $^+$ CD25 $^+$ T-cells from this region displayed the characteristic regulatory cell phenotype and exhibited suppressive activity. Moreover, an inverse correlation between CD4 $^+$ CD25 $^+$ T-cells and CD8 $^+$ cells in the liver of these patients

Fig. 3. CD4 $^+$ CD25 $^+$ T-cells in peri-tumor regions of the liver with HCC exhibit a regulatory phenotype. Lymphocytes were obtained from marginal regions of HCC (Peri-tumor) and peripheral blood (Blood) from a representative patient with HCC. The liver biopsy and peripheral blood samples were obtained from a representative patient with chronic hepatitis without HCC. Cells were stained with CD4, CD25, and CD152 (CTLA-4) (A) or CD45RA (B) or glucocorticoid-induced TNF receptor (GITR) (C). Then, CD4 $^+$ CD25 $^+$ cells were gated and analyzed. Numbers indicate the percentages in corresponding areas.

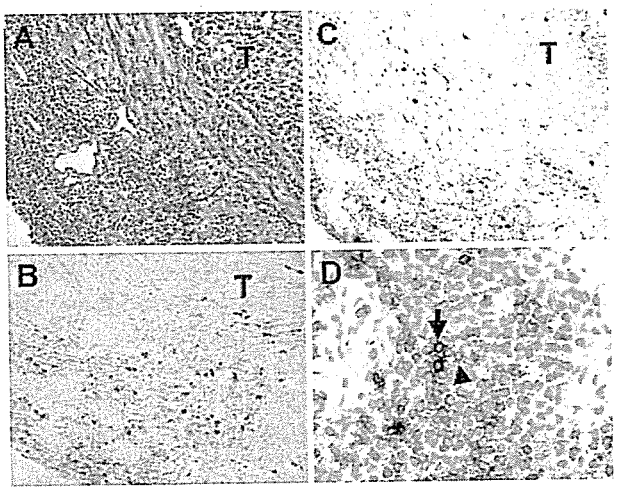

Fig. 4. Immunohistochemical detection of CD4 $^+$ CD25 $^+$ T-cells in the peri-tumor region of HCC. (A) Hematoxylin-Eosin staining (×100) shows many infiltrating cells around well-differentiated HCC. (B) Immunohistochemical staining (×100) for CD25 (brown-substrate) of the serial section shows many CD25 $^+$ cells among the infiltrating cells around the tumor. (C) Simultaneous staining for CD4 (blue-substrate) and CD25 (brown-substrate) of the serial section, and (D) higher magnification (×400) of the simultaneous staining for CD4 and CD25. Many CD4 $^+$ CD25 $^+$ double-positive cells detected as black cells (arrow) are seen among the infiltrating cells around the tumor. CD4 $^+$ CD25 $^-$ cells detected as blue cells (arrowhead) are scattered in the region. T, tumor. (For interpretation of the reference to colour in this legend, the reader is referred to the web version of this article).

suggested that these Treg cells inhibit CD8 $^+$ T-cell proliferation. To date there have been only a few reports showing an increase of CD4 $^+$ CD25 $^+$ Treg cells in TIL or in organs containing tumors. Woo et al. reported that CD4 $^+$ CD25 $^+$ T-cells existed in high proportions in TILs of patients with lung cancer [18,19], and that CD4 $^+$ CD25 $^+$ T-cells isolated from tumors strongly inhibited the proliferation of autologous PB T-cells stimulated by anti-CD3 [19]. CD4 $^+$ CD25 $^+$ T-cells isolated from the liver of patients with HCC have similar suppressive activity. Although, a tumor-specific antigen

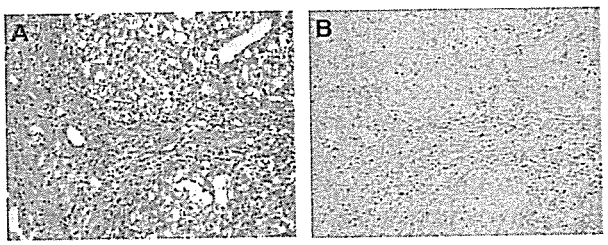

Fig. 5. Immunohistochemical detection of CD4 $^+$ CD25 $^+$ T-cells in the non-tumor region of HCC. Staining was performed using a distant area from HCC in the liver of the same patient as Fig. 4. (A) Hematoxylin-Eosin staining (×100). (B) Immunohistochemical staining (×100) for CD25 (brown-substrate) of non-tumor region shows that CD25-positive cells are scattered among the infiltrating cells. T, tumor. (For interpretation of the reference to colour in this legend, the reader is referred to the web version of this article).

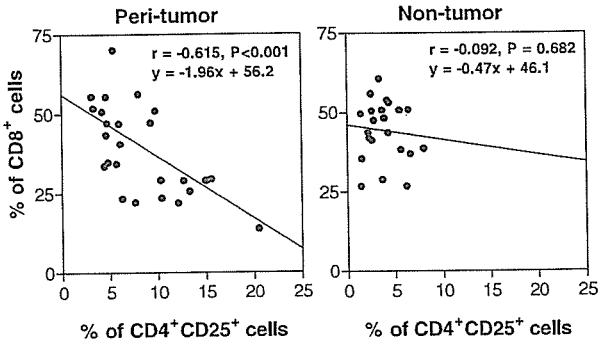

Fig. 6. Relationship between CD8 $^+$ cells and CD4 $^+$ CD25 $^+$ T-cells in the liver with HCC. Each plot shows the percentages of CD4 $^+$ CD25 $^+$ T-cells and CD8 $^+$ cells in each case among intrahepatic lymphocytes in the peri-tumor or non-tumor regions of the liver with HCC.

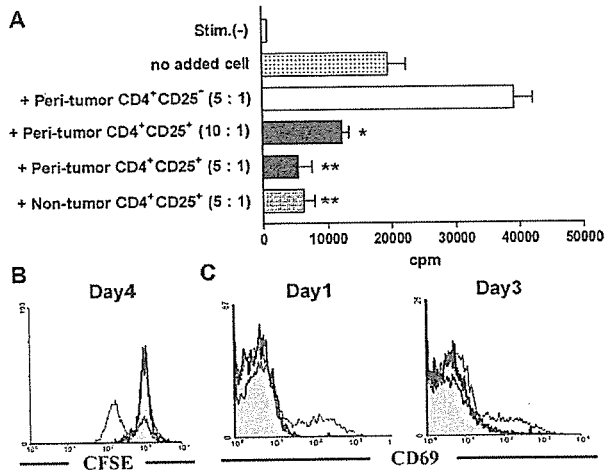

Fig. 7. CD4 $^+$ CD25 $^+$ T-cells obtained from the peri-tumor regions of HCC suppress autologous T-cell proliferation and activation of CD8 $^+$ T-cells stimulated with anti-CD3 and anti-CD28. (A) Autologous T-cells were stimulated with immobilized anti-CD3 and anti-CD28 in the presence or absence of indicated numbers of CD4 $^+$ CD25 $^+$ or CD4 $^+$ CD25 $^-$ T-cells obtained from peri-tumor regions or non-tumor regions of HCC. [^{3}H]Thymidine incorporation was measured during the last 18 h of a 4-day culture. Results are expressed as means of triplicate cultures (±SD) for one of five independent experiments performed on different donors, each with similar results. (B) Autologous CD3 $^+$ cells separated from PBL were labeled with CFSE, and cultured for 4 days without stimulation [gray shaded area] or with immobilized anti-CD3 and anti-CD28 in the presence [thick line] or absence [thin line] of CD4 $^+$ CD25 $^+$ T-cells obtained from peri-tumor regions of HCC. Cell division of CD8 $^+$ cells was analyzed by flow cytometry. These results shown are representative of three similar experiments performed on different donors. (C) Autologous CD3 $^+$ cells were separated from PBL, and cultured for 1 day or 3 days without stimulation [gray shaded area] or with immobilized anti-CD3 and anti-CD28 in the presence [thick line] or absence [thin line] of CD4 $^+$ CD25 $^+$ T-cells obtained from peri-tumor regions of HCC. CD69 expression on CD8 $^+$ cells was analyzed by flow cytometry. These results shown are representative of five similar experiments performed on different donors.

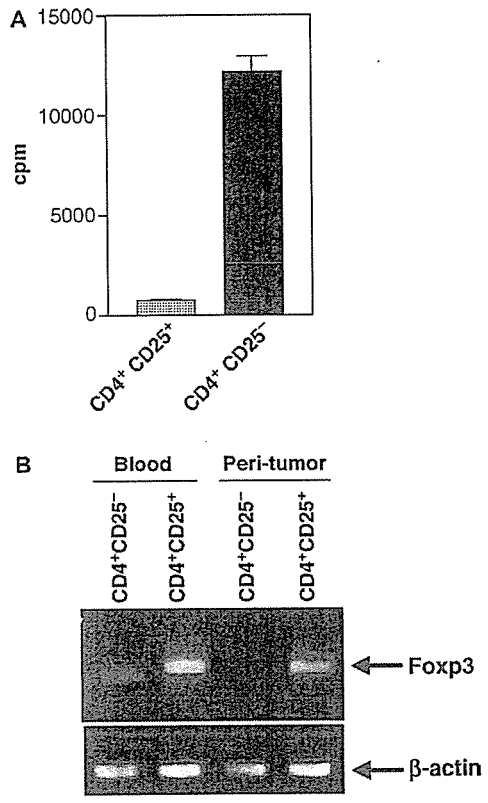

Fig. 8. $CD4^+CD25^+$ T-cells obtained from the peri-tumor regions of HCC showed a hyporesponsiveness to anti-CD3 stimulation, and expressed Foxp3 mRNA. (A) $CD4^+CD25^+$ and $CD4^+CD25^-$ T-cells were obtained from peri-tumor regions of HCC, and stimulated by anti-CD3 plus anti-CD28 mAb. [^{3}H]Thymidine incorporation was measured during the last 18 h of a 4-day culture. Results are expressed as means of triplicate cultures (±SD) for one of five independent experiments performed on different donors, each with similar results. (B) RT-PCR analysis of Foxp3 mRNA expression of $CD4^+CD25^+$ and $CD4^+CD25^-$ T-cells isolated from peripheral blood and the peri-tumor regions of HCC. As control, β-actin mRNA content was analyzed by RT-PCR in the same samples. One representative experiment out of five performed on different donors is shown.

would be a more suitable substrate, we used non-specific but conventional stimuli for induction of lymphocyte proliferation without adding IL-2. We could not exclude the possibility that $CD4^+CD25^+$ T-cells might simply act as a very effective in vitro sink for IL-2 critically needed for proliferation of $CD8^+$ T-cells.

$CD4^+CD25^+$ T-cells have been reported to be increased in the PB of patients with various cancers [15–17]. Sasada et al. described a significant increase of $CD4^+CD25^+$ T-cells in the PB of patients with 'liver carcinoma', but the histology of the tumors was not described [17]. A significant increase of $CD4^+CD25^+$ T-cells in the PB of patients with HCC has been reported recently [26], but this subset was decreased in our patients with HCC. Their series might have included patients with recurrent disease, whereas in the present study such patients were excluded. The discrepancy between our data and theirs may therefore have resulted from differences in the patient profile and disease stage. Unitt et al. recently showed that $CD4^+CD25^+Foxp3^+$ Treg cells were increased in TILs in HCC, and exceeded the proportion present in distant non-tumor tissues [27]. The Treg cells isolated from HCC have been shown to suppress the proliferation of autologous $CD8^+$ T-cells. A slight decrease in the proportion of circulating $CD4^+CD25^+$ Treg cells was also observed in HCC patients when compared with healthy individuals [27]. Although, we detected the increase of $CD4^+CD25^+$ T-cells in the marginal regions of HCC rather than in TILs, our present results were consistent with their observations. The decreased proportion of $CD4^+CD25^+$ T-cells in the PB of patients with HCC could possibly result from increased migration of Treg cells to the marginal regions of the tumor.

$CD4^+CD25^+$ Treg cells found in HCC could be natural, thymus-derived cells or suppressor cells with a similar phenotype induced in the periphery. As stated above, we have reported that TGF-β induces naive $CD4^+$ cells to become $CD25^+$ regulatory cells that have properties indistinguishable from natural $CD4^+CD25^+$ Treg cells [10,28]. These $CD4^+CD25^+$ Treg cells prevented $CD8^+$ T-cells from proliferating in response to alloantigens and from becoming cytotoxic effector cells [10]. Like natural $CD4^+CD25^+$ Treg cells, those induced with TGF-β express high levels of Foxp3 [29]. Moreover, others have reported that TGF-β up-regulates Foxp3 expression [30]. Foxp3 is a forkhead/winged helix transcription factor that is disrupted in Scurfy mouse and in the human immune dysregulation polyendocrinopathy enteropathy X-linked syndrome, both lacking natural $CD4^+CD25^+$ Treg cells [31–33]. Foxp3 is now recognized as a master control gene for the development and function of Treg cells [25]. In this study, we revealed Foxp3 mRNA expression of the $CD4^+CD25^+$ T-cells isolated from the liver of patients with HCC.

TGF-β levels in the plasma of HCC patients is increased [34]. Expression of this cytokine is also increased in the tumor [35,36]. In the present study, we confirmed by immunohistochemistry that TGF-β expressed in the liver with HCC was increased (results not shown). This result, taken together with our previous observations, suggests that the lack of effective tumor immunity in patients with HCC is not due to a lack of immunogenicity. Instead, $CD4^+$ T-cells activated by HCC-associated antigens in the presence of TGF-β could become $CD4^+CD25^+$ Treg cells. These cells, in turn, inhibit the activation of tumor-specific $CD8^+$ T-cells that accumulate at the margin of HCC so that they are unable to develop cytotoxic activity. The strong inverse correlation between $CD8^+$ cells

and $CD4^+CD25^+$ T-cells in the marginal regions of HCC supports this suggestion.

In summary, our observations provide additional insight into the regulatory mechanisms responsible for immunosuppression in HCC. As has been demonstrated in animal models, depletion of $CD4^+CD25^+$ Treg cells could be an effective strategy for enhancing tumor immunity especially in combination with attempts to augment the immunogenicity of tumor cells using vaccination of patients with tumor antigens or with antigen-pulsed dendritic cells (DC) [37,38]. Although, DC pulsed with various HCC-associated antigens have shown to suppress the tumor growth in animal models [39,40], further improvement of efficacy of the therapy must be necessary for their use in human trials [41]. In conclusion, manipulation of $CD4^+CD25^+$ Treg cells in terms of their frequency and functional activity could be one of the therapeutic measures for enhancing tumor immunity against HCC.

Acknowledgements

We would like to thank N. Honda for his excellent technical assistance. This work was supported in part by grants from the Ministry of Education, Culture, Sports, Science and Technology (MEXT), Japan, and the Japan Society for the Promotion of Science (JSPS).

References

[1] Shevach EM. Regulatory T cells in autoimmunity. Annu Rev Immunol 2000;18:423–449.
[2] Sakaguchi S. Regulatory T cells: key controllers of immunologic self-tolerance. Cell 2000;101:455–458.
[3] Bach JF. Regulatory T cells under scrutiny. Nat Rev Immunol 2003;3:189–198.
[4] Shevach EM. Certified professionals: $CD4^+CD25^+$ suppressor T cells. J Exp Med 2001;193:F41–F46.
[5] Stephens LA, Mottet C, Mason D, Powrie F. Human $CD4^+CD25^+$ thymocytes and peripheral T cells have immune suppressive activity in vitro. Eur J Immunol 2001;31:1247–1254.
[6] Jonuleit H, Schmitt E, Stassen M, Tuettenberg A, Knop J, Enk AH. Identification and functional characterization of human $CD4^+CD25^+$ T cells with regulatory properties isolated from peripheral blood. J Exp Med 2001;193:1285–1294.
[7] Shevach EM. $CD4^+CD25^+$ suppressor T cells: more questions than answers. Nat Rev Immunol 2002;2:389–400.
[8] Jordan MS, Boesteanu A, Reed AJ, Petrone AL, Holenbeck AE, Lerman MA, et al. Thymic selection of $CD4^+CD25^+$ regulatory T cells induced by an agonist self-peptide. Nat Immunol 2001;2:301–306.
[9] Diechman D, Plottner H, Berchtold S, Berger T, Schuler G. Ex vivo isolation and characterization of $CD4^+CD25^+$ T cells with regulatory properties from human blood. J Exp Med 2001;193:1303–1310.
[10] Yamagiwa S, Gray JD, Hashimoto S, Horwitz DA. A role for TGF-β in the generation and expansion of $CD4^+CD25^+$ regulatory T cells from human peripheral blood. J Immunol 2001;166:7282–7289.
[11] Morse MA, Clay TM, Mosca P, Lyerly HK. Immunoregulatory T cells in cancer immunotherapy. Expert Opin Biol Ther 2002;2:827–834.
[12] Jones E, Dahm-Vicker M, Golgher D, Gallimore A. $CD25^+$ regulatory T cells and tumor immunity. Immunol Lett 2003;85:141–143.
[13] Shimizu J, Yamazaki S, Sakaguchi S. Induction of tumor immunity by removing $CD25^+CD4^+$ T cells: a common basis between tumor immunity and autoimmunity. J Immunol 1999;163:5211–5218.
[14] Onizuka S, Tawara I, Shimizu J, Sakaguchi S, Fujita T, Nakayama E. Tumor rejection by in vivo administration of anti-CD25 (interleukin-2 receptor alpha) monoclonal antibody. Cancer Res 1999;59:3128–3133.
[15] Somasundaram R, Jacob L, Swoboda R, Caputo L, Song H, Basak S, et al. Inhibition of cytolytic T lymphocyte proliferation by autologous $CD4^+/CD25^+$ regulatory T cells in a colorectal carcinoma patients is mediated by transforming growth factor-β. Cancer Res 2002;62:5267–7272.
[16] Wolf AM, Wolf D, Steurer M, Gastl G, Gunsilius E, Grubeck-Loebenstein B. Increase of regulatory T cells in the peripheral blood of cancer patients. Clin Cancer Res 2003;9:606–612.
[17] Sasada T, Kimura M, Yoshida Y, Kanai M, Takabayashi A. $CD4^+CD25^+$ regulatory T cells in patients with gastrointestinal malignancies. Possible involvement of regulatory T cells in disease progression. Cancer 2003;98:1089–1099.
[18] Woo EY, Chu CS, Goletz TJ, Schlienger K, Yeh H, Coukos G, et al. Regulatory $CD4^+CD25^+$ T cells in tumors from patients with early-stage non-small cell lung cancer and late-stage ovarian cancer. Cancer Res 2001;61:4766–4772.
[19] Woo EY, Yeh H, Chu CS, Schlienger K, Carroll RG, Riley JL, et al. Regulatory T cells from lung cancer patients directly inhibit autologous T cell proliferation. J Immunol 2002;168:4272–4276.
[20] Cureil TJ, Coukos G, Zou L, Alvarez X, Cheng P, Mottram P, et al. Specific recruitment of regulatory T cells in ovarian carcinoma fosters immune privilege and predicts reduced survival. Nat Med 2004;10:942–949.
[21] Kita H, Mackay IR, van de Water J, Gershwin ME. The lymphoid liver: considerations on pathways to autoimmune injury. Hepatology 2001;120:1485–1501.
[22] Norris S, Collins C, Doherty DG, Smith F, McEntee G, Traynor O, et al. Resident human hepatic lymphocytes are phenotypically different from circulating lymphocytes. J Hepatol 1998;28: 84–90.
[23] Doherty DG, Norris S, Madrigal-Estebas L, McEntee G, Traynor O, Hegarty JE, et al. The human liver contains multiple populations of NK cells, T cells and $CD3^+CD56^+$ natural T cells with distinct cytotoxic activities and Th1, Th2 and Th0 cytokine secretion patterns. J Immunol 1999;163:2314–2321.
[24] Verhasselt V, Vosters O, Beuneu C, Nicaise C, Stordeur P, Goldman M. Induction of FOXP3-expressing regulatory $CD4^{pos}$ T cells by human mature autologous dendritic cells. Eur J Immunol 2004;34:762–772.
[25] Ramsdell F. Foxp3 and natural regulatory T cells: key to a cell lineage?. Immunity 2003;19:165–168.
[26] Ormandy LA, Hillemann T, Wedemeyer H, Manns MP, Greten TF, Korangy F. Increased populations of regulatory T cells in peripheral blood of patients wit hepatocellular carcinoma. Cancer Res 2005;65:2457–2464.
[27] Unitt E, Rushbrook SM, Marshall A, Davies S, Gibbs P, Morris LS, et al. Compromised lymphocytes infiltrate hepatocellular carcinoma: the role of T-regulatory cells. Hepatology 2005;41:722–730.
[28] Horwitz DA, Zheng SG, Gray JD. The role of the combination of IL-2 and TGF-β or IL-10 in the generation and function of $CD4^+CD25^+$ and $CD8^+$ regulatory T cell subsets. J Leukoc Biol 2003;74:471–478.

[29] Zheng SG, Wang JH, Koss MN, Quismorio Jr F, Gray JD, Horwitz DA. $CD4^+$ and $CD8^+$ regulatory T cells generated ex vivo with IL-2 and TGF-beta suppress a stimulatory graft-versus-host disease with a lupus-like syndrome. J Immunol 2004;172:1531–1539.
[30] Chen W, Jin W, Hardegen N, Lei KJ, Li L, Marinos N, et al. Conversion of peripheral $CD4^+CD25^-$ naive T cells to $CD4^+CD25^+$ regulatory T cells by TGF-beta induction of transcription factor Foxp3. J Exp Med 2003;198:1875–1886.
[31] Hori S, Nomura T, Sakaguchi S. Control of regulatory T cell development by the transcription factor Foxp3. Science 2003;299:1057–1061.
[32] Khattri R, Cox T, Yasayko SA, Ramsdell F. An essential role for Scurfin in $CD4^+CD25^+$ T regulatory cells. Nat Immunol 2003;4:337–342.
[33] Fontenot JD, Gavin MA, Rudensky AY. Foxp3 programs the development and function $CD4^+CD25^+$ regulatory T cells. Nat Immunol 2003;4:330–336.
[34] Shirai Y, Kawata S, Tamura S, Ito N, Tsusima H, Takahashi K, et al. Plasma transforming growth factor-β1 in patients with hepatocellular carcinoma. Cancer 1994;73:2275–2279.
[35] Bedossa P, Peltier E, Terris B, Franco D, Poynard T. Transforming growth factor-β1 (TGF-β1) and TGF-β1 receptors in normal, cirrhotic, and neoplastic human livers. Hepatology 1995;21:760–766.
[36] Abou-Shady M, Baer HU, Friess H, Berberat P, Zimmermann A, Graber H, et al. Transforming growth factor betas and their signaling receptors in human hepatocellular carcinoma. Am J Surg 1999;177:209–215.
[37] Sutmuller RP, van Duivenvoorde LM, van Elsas A, Schumacher TN, Wildenberg ME, Allison JP, et al. Synergism of cytotoxic T lymphocyte-associated antigen 4 blockade and depletion of $CD25^+$ regulatory T cells in antitumor therapy reveals alternative pathways for suppression of autoreactive cytotoxic T lymphocyte responses. J Exp Med 2001;194:823–832.
[38] Steitz J, Bruck J, Lenz J, Knop J, Tuting T. Depletion of $CD25^+CD4^+$ T cells and treatment with tyrosinase-related protein 2-transduced dendritic cells enhance the interferon α-induced $CD8^+$ T-cell-dependent immune defense of B16 melanoma. Cancer Res 1999;59:3128–3133.
[39] Shibolet O, Alper R, Zlotogarov L, Thalenfeld B, Engelhardt D, Rabbani E, et al. NKT and CD8 lymphocytes mediate suppression of hepatocellular carcinoma growth via tumor antigen-pulsed dendritic cells. Int J Cancer 2003;106:236–243.
[40] Irie M, Homma S, Komita H, Zeniya M, Kufe D, Ohno T, et al. Inhibition of spontaneous development of liver tumors by inoculation with dendritic cells loaded with hepatocellular carcinoma cells in C3H/HeNCRJ mice. Int J Cancer 2004;111:238–245.
[41] Ladhams A, Schmidt C, Sing G, Butterworth L, Fielding G, Tesar P, et al. Treatment of non-resectable hepatocellular carcinoma with autologous tumor-pulsed dendritic cells. J Gastroenterol Hepatol 2002;17:889–896.

PO Box 2345, Beijing 100023, China
www.wjgnet.com
wjg@wjgnet.com

World J Gastroenterol 2006 April 7; 12(13):2075-2079
World Journal of Gastroenterology ISSN 1007-9327

RAPID COMMUNICATION

Prognosis following transcatheter arterial embolization for 121 patients with unresectable hepatocellular carcinoma with or without a history of treatment

Atsushi Hiraoka, Teru Kumagi, Masashi Hirooka, Takahide Uehara, Kiyotaka Kurose, Hidehito Iuchi, Yoichi Hiasa, Bunzo Matsuura, Kojiro Michitaka, Seishi Kumano, Hiroaki Tanaka, Yoshimasa Yamashita, Norio Horiike, Teruhito Mochizuki, Morikazu Onji

Atsushi Hiraoka, Teru Kumagi, Masashi Hirooka, Takahide Uehara, Kiyotaka Kurose, Hidehito Iuchi, Yoichi Hiasa, Bunzo Matsuura, Kojiro Michitaka, Norio Horiike, Morikazu Onji, Third Department of Internal Medicine, Ehime University School of Medicine, Ehime, Japan
Kojiro Michitaka, Endoscopy Center, Ehime University School of Medicine, Ehime, Japan
Seishi Kumano, Hiroaki Tanaka, Teruhito Mochizuki, Department of Radiology, Ehime University School of Medicine, Ehime, Japan
Yoshimasa Yamashita, Department of Internal Medicine, Ehime Prefecture Central Hospital, Ehime, Japan
Correspondence to: Morikazu Onji, MD, Third Department of Internal Medicine, Ehime University School of Medicine, Ehime 791-0295, Japan. onjimori@m.ehime-u.ac.jp
Telephone: +81-89-9605308 Fax: +81-89-9605310
Received: 2005-09-11 Accepted: 2005-10-26

Abstract

AIM: To retrospectively evaluate the prognosis of patients with hepatocellular carcinoma (HCC) with or without a history of therapy for HCC following transcatheter arterial embolization (TAE).

METHODS: One hundred and twenty-one patients with HCC treated with TAE from 1992 to 2004 in our hospital were enrolled in this study. Eighty-four patients had a history of treatment for HCC, while 37 did not. At the time of entry, patients with extra-hepatic metastasis, portal vein tumor thrombosis, or Child-Pugh class C were excluded. TAE was repeated when recurrence of HCC was diagnosed by elevated tumor markers, or ultrasonography or dynamic computed tomography findings.

RESULTS: Tumor size was larger and the number of tumors was fewer in patients without past treatment ($P<0.01$). However, there were no differences in tumor node metastasis (TNM) stage or survival rate between the 2 groups. A bilobular tumor and high level of α-fetoprotein (AFP) (>100 ng/mL) were factors related to a poor prognosis in patients with a history of HCC.

CONCLUSION: The prognosis following TAE is similar between HCC patients with and without past treatment. Early diagnosis of HCC or recurrent HCC and obtaining good local control against HCC before entry to a repeated TAE course can improve prognosis.

Key words: Unresectable hepatocellular carcinoma; Prognosis; Repeated transcatheter arterial embolization

Hiraoka A, Kumagi T, Hirooka M, Uehara T, Kurose K, Iuchi H, Hiasa Y, Matsuura B, Michitaka K, Kumano S, Tanaka H, Yamashita Y, Horiike N, Mochizuki T, Onji M. Prognosis following transcatheter arterial embolization for 121 patients with unresectable hepatocellular carcinoma with or without a history of treatment. *World J Gastroenterol* 2006; 12(13): 2075-2079

http://www.wjgnet.com/1007-9327/12/2075.asp

INTRODUCTION

Liver transplantation is recognized as an effective therapy for hepatocellular carcinoma (HCC)[1]. However, a shortage of donors in Japan has led to the general use of transcatheter arterial embolization and transcatheter arterial chemoembolization (TAE) in patients with unresectable HCC without an indication of surgery and percutaneous therapy. Although disappointing results are published[2-4], the usefulness of TAE has been reconfirmed recently as some studies found that the procedure reduces the overall 2-year mortality rate and improves the survival rate of patients with unresectable HCC[5-8]. Past reports regarding the prognosis of patients with HCC are usually limited to the initial therapy, including surgery[9], percutaneous ethanol injection therapy (PEIT)[10], radiofrequency ablation (RFA)[11,12], and TAE. In previous studies of TAE, the subjects had no history of treatment for HCC. However, most patients with HCC have no indication for therapy such as surgery, PEIT and RFA due to multiple recurrences finally. No reports have evaluated prognosis and its related factors of patients with a history of HCC following a repeated TAE course. In the present study, we retrospectively evaluated the prognosis of HCC patients with or without a history of therapy for HCC following TAE.

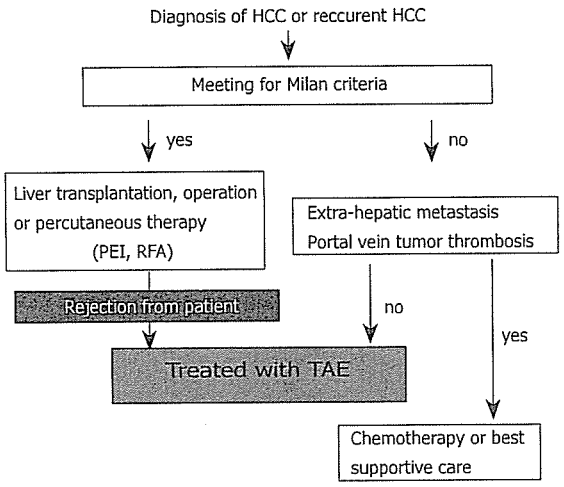

Figure 1 Strategy for treatment of HCC employed at our institution. Nearly all patients with HCC, which were outside of the Milan criteria, were recommended for a repeated TAE course.

MATERIALS AND METHODS

This was a single-center retrospective study conducted at Ehime University Hospital. One hundred and twenty-one patients with advanced HCC treated with TAE from 1992 to 2004 were enrolled in the study. After informed consent was obtained, the entry date was considered the day of the first TAE therapy after enrollment. The diagnosis of HCC was based on histological and cytologic findings or findings of dynamic computed tomography (CT). Tumor stage was established by dynamic CT, ultrasonography (US), angiography, chest CT, and bone scintigraphy examinations.

Patients with extra-hepatic metastasis, portal vein tumor thrombosis (PVTT), or Child-Pugh class C at entry were excluded from this study since the existence of PVTT and a high Child-Pugh score are poor prognostic markers and TAE can not improve these patients[5]. As a result, 37 patients with no history of treatment for HCC and 84 with such a history of surgery, PEIT, or RFA, were studied. During the 13-year study period, a total of 121 patients underwent 435 courses of TAE, with 99 (82%) outside of the Milan criteria[1]. In 37% of 121 patients, HCC was confirmed by histological examination. Others were diagnosed based on the increasing course of α-fetoprotein (AFP) and dynamic CT. All HCC nodules treated with TAE were hypervascular.

The patients treated with TAE were evaluated based on our strategy (Figure 1). TAE was repeated when HCC recurrence was diagnosed by the elevation of tumor markers, or US or dynamic CT examination findings. Experienced radiologists performed all the TAE procedures. A microcatheter was inserted into the artery feeding the tumor super-selectively after conventional hepatic angiography or angiography CT, and then a segmental or subsegmental TAE procedure[13] was performed. Before the procedure, antegrade flow in the portal vein and no obstruction of the main trunk of the portal vein were confirmed by US, dynamic CT, and portography findings via the superior mesenteric artery. Lipiodol and a gelatin sponge (Gelfoam, Upjohn, Kalamazoo, MI, USA) were used for embolization, and epirubicin hydrochloride was used together with Lipiodol in 25% of the cases. The goal of embolization was disappearance of tumor staining without complete obstruction of the hepatic artery. Patients that underwent additional chemotherapy via a subcutaneously implanted injection port, surgery, PEIT, or RFA for the purpose of reducing the size of the tumor after undergoing TAE were excluded from this study.

Table 1 Backgrounds of patients without or with history of treatment

	Patients without history of HCC (n=37)	Patients with history of HCC (n=84)	P value
Age (yr)	66.4 ± 9.9	67.0 ± 8.1	NS
Sex (male : female)	32 : 5	64 : 20	NS
Frequency of positive for anti-HCV	72%	81%	NS
TNM stage (II : III)	12 : 25	35 : 49	NS
Tumor size (mm)	46.4 ± 23.5	27.7 ± 16.1	P<0.01
Number of tumors (≤3 : >3)	21 : 16	23 : 61	P<0.01
Monolobular : bilobular	17 : 20	27 : 57	NS
Child-Pugh class (A : B)	27 : 10	48 : 36	NS
Alanine transferase (IU/L)	63.8 ± 45.1	82.1 ± 64.3	P=0.07
AFP (≤100 : >100 ng/mL)	23 : 14	53 : 31	NS
TAE with or without anti-cancer medication	13 : 24	17 : 67	NS
Average number of past treatments	-	2.9 ± 2.2	-
History of hepatectomy	-	18%	-
Average observation period (d)	557.6 ± 377.0	493.6 ± 390.6	NS

Anti-HCV: hepatitis C virus antibody; AFP: α-fetoprotein; TNM stage: tumor node metastasis stage.

The backgrounds of both groups at study entry are shown in Table 1. The group of patients without past treatment consisted of 32 males and 5 females, of whom 12 and 25 patients were in tumor node metastasis (TNM) stage[14,15] II and III, respectively. Furthermore, 27 were Child-Pugh class A and 10 were class B, of whom 72% were positive for the hepatitis C virus antibody (anti-HCV) and 14% for the hepatitis B surface antigen (HBs Ag).

As for the group of patients with treatment history, 64 were male and 20 female, of whom 35 and 49 were TNM stages II and III, respectively. Forty-eight patients in this group were Child-Pugh class A and 36 class B, of whom 81% were positive for anti-HCV and 16% for HBs Ag.

Determination of markers of hepatitis viruses

The presence of anti-HCV and HBs Ag was determined precisely using enzyme immunoassay kits (Imcheck-FHCV, Kokusai-Shiyaku, Kobe, Japan; AxSYM HBs Ag, Dainabot, Tokyo, Japan), according to the manufacturer's instructions.

Statistical analysis

All statistical analyses were carried out using a personal computer with StatView version 5.0 (SAS Institute, Inc., Berkeley, CA, USA). Analyses were conducted using Student's t-test, Mann-Whitney U test, Cox's proportional hazards regression model, logrank test, and the Kaplan-Meier method. $P < 0.05$ was considered statistically significant.

Table 2 Univariate analysis of patients with past treatment for HCC (n=84)

Factors	Number	Hazard ratio	95% CI	*P* value
Age (= and <65 : >65)	38 : 46	0.99	0.95-1.02	NS
Sex (male : female)	64 : 20	1.02	0.54-1.93	NS
Anti-HCV (positive : negative)	67 : 17	1.31	0.64-2.67	NS
TNM stage (II : III)	35 : 49	1.57	0.83-3.00	NS
Tumor size (mm)	-	1	0.98-1.02	NS
Number of tumors (≤3 : >3)	23 : 61	0.88	0.47-1.67	NS
Monolobular : bilobular	27 : 57	2	1.04-3.86	$P<0.05$
Child-Pugh class (A : B)	48 : 36	1.07	0.59-1.95	NS
AFP (≤100 : >100 ng/mL)	53 : 31	1.9	1.03-3.48	$P<0.05$
History of hepatectomy (negative : positive)	69 : 15	1.63	0.72-3.70	NS
Number of past treatments	-	1.05	0.93-1.19	NS

CI: confidence interval; anti-HCV: hepatitis C virus antibody; AFP: α-fetoprotein; TNM stage: tumor node metastasis stage.

Table 3 Multivariate analysis of patients with past treatment for HCC (n=84)

Factors	Hazard ratio	95% CI	*P* value
Existence of bilobular tumors	2.37	1.19-4.71	$P<0.05$
AFP (>100 ng/mL)	2.24	1.19-4.23	$P<0.05$

CI: confidence interval; AFP: α-fetoprotein.

RESULTS

There were no significant differences in the background findings between patients with or without past treatments for HCC, except for tumor size and the number of tumors ($P<0.01$) (Table 1). There was also no significant difference in patient distribution for TNM staging between the groups. None of the patients died due to the TAE procedure. For patients with treatment history, the average number of past treatments for HCC was 2.9±2.2 (range 1-10) and a hepatectomy was performed before entry to the repeated TAE course in 18% of these patients.

The survival rate was not significantly different between the 2 groups (Figure 2). The 1-, 2-, and 3-year survival rates were 90%, 57%, and 20% respectively in patients without past treatment, and 75%, 43%, and 25% respectively in those with past treatment. The factors related to poor prognosis in the 84 patients with past treatment for HCC were evaluated. Seventy-four of them (88%) were outside of the Milan criteria. According to univariate analysis, variables significantly associated with survival were tumor location (bilobular) and a high concentration of AFP (>100 ng/mL) ($P<0.05$). There were no relationships between the prognosis of patients with a history of treatment for HCC and other factors, including history of past hepatectomy and the number of past treatments for HCC (Table 2). Multivariate analysis showed that the existence of bilobular HCC and high concentrations of AFP (>100 ng/mL) were the factors for poor prognosis ($P<0.05$, Table 3). The survival rate of patients without both risk factors was better than that of those with both risk factors ($P<0.01$, Figure 3). In all 121 patients, the existence of bilobular HCC was related to poor prognosis ($P<0.01$), while a high concentration of AFP ($P=0.059$) and other factors including past treatments, were not related to poor prognosis.

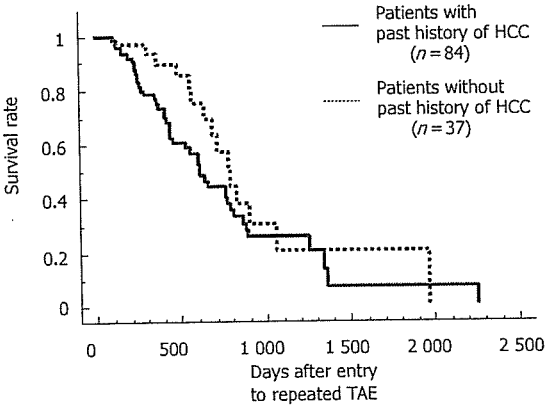

Figure 2 Survival rates of HCC patients with or without past treatment for HCC. There was no significant difference between the 2 groups. Survival rates after 1, 2, and 3 years were 90%, 57%, and 20% respectively for patients without past treatment, and 75%, 43%, and 25% respectively for patients with past treatment.

DISCUSSION

The prognosis of a patient with HCC is dependent on the hepatic reserve function and HCC staging[16,17]. A repeated TAE course is widely used for patients with unresectable HCC[18,19], though it was reported that TAE is not effective for improving the prognosis of such patients[2,3,4]. The reason for the disappointing results is that TAE is repeated within a fixed period of time although the liver reserves function and the patients have or have no recurrence of HCC. When TAE is repeated after a fixed period of time, embolization from the main trunk of the hepatic artery can lead to liver atrophy and deterioration of hepatic reserve function. Recently, the efficacy of TAE for patients with HCC has been reported, with good improvement of survival results[5-8]. Caturelli *et al*[20] reported that repeated TAE does not induce long-term deterioration of hepatic reserve function in HCC patients with Child-Pugh A and B but without PVTT.

Since repeated TAE for a fixed period without recurrence can lead to a reduction in hepatic reserve function, we think that it is important to perform TAE at the time

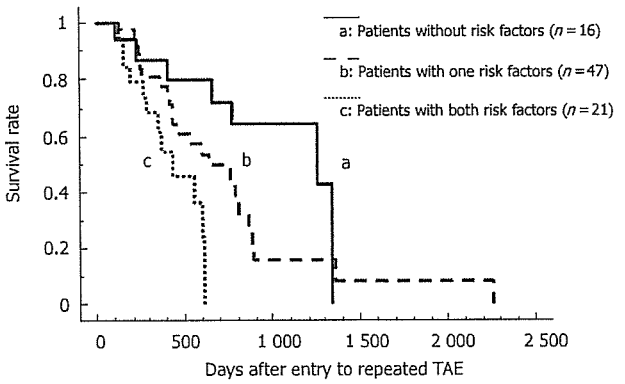

Figure 3 Survival rates of HCC patients with past treatment and with or without the 2 risk factors found in the present study. Significant differences were shown between "a" and "b" and between "b" and "c" ($P<0.01$ and $P=0.01$), while there were no significant differences between "a" and "b" ($P=0.08$). a: Patients without either factor [existence of bilobular tumors and high concentration of AFP (greater than 100 ng/mL; $n=16$)]; b: Patients with one of the factors ($n=47$); c: Patients with both factors ($n=21$).

when HCC recurrence is diagnosed by the elevation of tumor markers, or based on US or dynamic CT findings [21,22]. Recently, diagnostic progress of US and CT has made it easier to accurately diagnose new and recurrent HCC with low levels of AFP. Dynamic CT can offer detailed information about tumor vascularity and dynamic CT is useful to distinguish cholangiocarcinoma from HCC[23,24]. In our study metastatic liver tumor was denied from clinical course in all cases. In a large number of patients, HCC develops to an unresectable condition during the course of therapy and becomes outside of the Milan criteria. To our knowledge, the prognosis of patients with a history of HCC and factors for poor prognosis have not been reported after a repeated TAE course. In the present study, though the tumor maximum size and the number of tumors were different between the patients with or without past treatment, the survival rates of both groups after undergoing TAE did not show a significant difference, which might be due to no significant difference in TNM staging distribution between the groups.

As for the patients with past treatment, a past hepatectomy and the number of past percutaneous therapies (e.g. PEIT and RFA) did not influence the prognosis after repeated TAE in regard to maintaining liver reserve function. A high concentration of AFP and tumor location (bilobular) each had a significant influence. The elevation of AFP and existence of bilobular HCC are dependent on the malignant potential of HCC [25] and intra-hepatic metastasis, respectively.

Prognosis was not significantly different between HCC patients with or without a history of HCC following TAE. Our results show that diagnosis of HCC or recurrent HCC in the early stage and obtaining good local control against HCC before a repeated TAE course can reduce the time bias and improve prognosis.

REFERENCES

1 **Mazzaferro V,** Regalia E, Doci R, Andreola S, Pulvirenti A, Bozzetti F, Montalto F, Ammatuna M, Morabito A, Gennari L. Liver transplantation for the treatment of small hepatocellular carcinomas in patients with cirrhosis. *N Engl J Med* 1996; **334**: 693-699
2 A comparison of lipiodol chemoembolization and conservative treatment for unresectable hepatocellular carcinoma. Groupe d'Etude et de Traitement du Carcinome Hepatocellulaire. *N Engl J Med* 1995; **332**: 1256-1261
3 **Bruix J,** Llovet JM, Castells A, Montana X, Bru C, Ayuso MC, Vilana R, Rodes J. Transarterial embolization versus symptomatic treatment in patients with advanced hepatocellular carcinoma: results of a randomized, controlled trial in a single institution. *Hepatology* 1998; **27**: 1578-1583
4 **Pelletier G,** Ducreux M, Gay F, Luboinski M, Hagege H, Dao T, Van Steenbergen W, Buffet C, Rougier P, Adler M, Pignon JP, Roche A. Treatment of unresectable hepatocellular carcinoma with lipiodol chemoembolization: a multicenter randomized trial. Groupe CHC. *J Hepatol* 1998; **29**: 129-134
5 **Llad inverted question marko L,** Virgili J, Figueras J, Valls C, Dominguez J, Rafecas A, Torras J, Fabregat J, Guardiola J, Jaurrieta E. A prognostic index of the survival of patients with unresectable hepatocellular carcinoma after transcatheter arterial chemoembolization. *Cancer* 2000; **88**: 50-57
6 **Lo CM,** Ngan H, Tso WK, Liu CL, Lam CM, Poon RT, Fan ST, Wong J. Randomized controlled trial of transarterial lipiodol chemoembolization for unresectable hepatocellular carcinoma. *Hepatology* 2002; **35**: 1164-1171
7 **Llovet JM,** Real MI, Montana X, Planas R, Coll S, Aponte J, Ayuso C, Sala M, Muchart J, Sola R, Rodes J, Bruix J. Arterial embolisation or chemoembolisation versus symptomatic treatment in patients with unresectable hepatocellular carcinoma: a randomised controlled trial. *Lancet* 2002; **359**: 1734-1739
8 **Camma C,** Schepis F, Orlando A, Albanese M, Shahied L, Trevisani F, Andreone P, Craxi A, Cottone M. Transarterial chemoembolization for unresectable hepatocellular carcinoma: meta-analysis of randomized controlled trials. *Radiology* 2002; **224**: 47-54
9 **Takayama T,** Makuuchi M. Surgical resection. Diagnosis and Treatment of Hepatocellular Carcinoma, ed by T Livraghi, M Makuuchi, Greenwich Medical Media, London, 1997: 279-294
10 **Livraghi T,** Bolondi L, Lazzaroni S, Marin G, Morabito A, Rapaccini GL, Salmi A, Torzilli G. Percutaneous ethanol injection in the treatment of hepatocellular carcinoma in cirrhosis. A study on 207 patients. *Cancer* 1992; **69**: 925-929
11 **Kudo M.** Local ablation therapy for hepatocellular carcinoma: current status and future perspectives. *J Gastroenterol* 2004; **39**: 205-214
12 **Rossi S,** Buscarini E, Garbagnati F, Di Stasi M, Quaretti P, Rago M, Zangrandi A, Andreola S, Silverman D, Buscarini L. Percutaneous treatment of small hepatic tumors by an expandable RF needle electrode. *AJR Am J Roentgenol* 1998; **170**: 1015-1022
13 **Matsui O,** Kadoya M, Yoshikawa J, Gabata T, Takashima T, Demachi H. Subsegmental transcatheter arterial embolization for small hepatocellular carcinomas: local therapeutic effect and 5-year survival rate. *Cancer Chemother Pharmacol* 1994; **33 Suppl**: S84-S88
14 **Liver Cancer Study Group of Japan.** The general rules for the clinical and pathological study of primary liver cancer (in Japanese), 4th ed. Kanehara, Tokyo, 2000: 19
15 **Kudo M,** Chung H, Haji S, Osaki Y, Oka H, Seki T, Kasugai H, Sasaki Y, Matsunaga T. Validation of a new prognostic staging system for hepatocellular carcinoma: the JIS score compared with the CLIP score. *Hepatology* 2004; **40**: 1396-1405
16 **Arii S,** Yamaoka Y, Futagawa S, Inoue K, Kobayashi K, Kojiro M, Makuuchi M, Nakamura Y, Okita K, Yamada R. Results of surgical and nonsurgical treatment for small-sized hepatocellular carcinomas: a retrospective and nationwide survey in Japan. The Liver Cancer Study Group of Japan. *Hepatology* 2000; **32**: 1224-1229
17 **Kudo M,** Chung H, Osaki Y. Prognostic staging system for hepatocellular carcinoma (CLIP score): its value and limitations, and a proposal for a new staging system, the Japan Integrated

Staging Score (JIS score). *J Gastroenterol* 2003; 38: 207-215
18 **Ikeda K**, Kumada H, Saitoh S, Arase Y, Chayama K. Effect of repeated transcatheter arterial embolization on the survival time in patients with hepatocellular carcinoma. An analysis by the Cox proportional hazard model. *Cancer* 1991; 68: 2150-2154
19 **Hatanaka Y**, Yamashita Y, Takahashi M, Koga Y, Saito R, Nakashima K, Urata J, Miyao M. Unresectable hepatocellular carcinoma: analysis of prognostic factors in transcatheter management. *Radiology* 1995; **195**: 747-752
20 **Caturelli E**, Siena DA, Fusilli S, Villani MR, Schiavone G, Nardella M, Balzano S, Florio F. Transcatheter arterial chemoembolization for hepatocellular carcinoma in patients with cirrhosis: evaluation of damage to nontumorous liver tissue-long-term prospective study. *Radiology* 2000; **215**: 123-128
21 **Chalasani N**, Horlander JC Sr, Said A, Hoen H, Kopecky KK, Stockberger SM Jr, Manam R, Kwo PY, Lumeng L. Screening for hepatocellular carcinoma in patients with advanced cirrhosis. *Am J Gastroenterol* 1999; **94**: 2988-2993
22 **Lim JH**, Kim CK, Lee WJ, Park CK, Koh KC, Paik SW, Joh JW. Detection of hepatocellular carcinomas and dysplastic nodules in cirrhotic livers: accuracy of helical CT in transplant patients. *AJR Am J Roentgenol* 2000; **175**: 693-698
23 **Honda H**, Onitsuka H, Yasumori K, Hayashi T, Ochiai K, Gibo M, Adachi E, Matsumata T, Masuda K. Intrahepatic peripheral cholangiocarcinoma: two-phased dynamic incremental CT and pathologic correlation. *J Comput Assist Tomogr* 1993; **17**: 397-402
24 **Lacomis JM**, Baron RL, Oliver JH 3rd, Nalesnik MA, Federle MP. Cholangiocarcinoma: delayed CT contrast enhancement patterns. *Radiology* 1997; **203**: 98-104
25 **Peng SY**, Lai PL, Chu JS, Lee PH, Tsung PT, Chen DS, Hsu HC. Expression and hypomethylation of alpha-fetoprotein gene in unicentric and multicentric human hepatocellular carcinomas. *Hepatology* 1993; **17**: 35-41

S- Editor Wang J **L- Editor** Wang XL **E- Editor** Ma WH

Virtual Sonographic Radiofrequency Ablation of Hepatocellular Carcinoma Visualized on CT but Not on Conventional Sonography

Masashi Hirooka[1]
Hidehito Iuchi
Teru Kumagi
Shuichiro Shigematsu
Atsushi Hiraoka
Takahide Uehara
Kiyotaka Kurose
Norio Horiike
Morikazu Onji

OBJECTIVE. Some nodules cannot be visualized clearly on conventional sonography but can be visualized on CT. In the present study, we evaluated the usefulness of real-time percutaneous ablation therapy under virtual sonographic guidance for these nodules.

SUBJECTS AND METHODS. In vitro experiments were performed with gelatin gel to evaluate the accuracy of virtual sonography. We also studied 50 patients with 58 hepatocellular carcinoma nodules, of whom 18 patients (21 nodules) underwent radiofrequency ablation by virtual sonography. This was the initial treatment for seven of these patients and an additional treatment for 11 patients. Thirty-two patients (37 nodules) received radiofrequency ablation without virtual imaging. The patients receiving standard radiofrequency ablation were retrospectively selected as the historical control group under the same conditions as the study group.

RESULTS. The in vitro gelatin gel study revealed that all punctures had been performed accurately. In both the initial-treatment group and the additional-treatment group, the mean number of treatments with virtual sonography was significantly lower than that without virtual sonography ($p = 0.003$ for both groups). The rates of local recurrence and complications did not differ significantly between the two groups.

CONCLUSION. In the treatment of nodules not depicted on sonography, radiofrequency ablation assisted by virtual sonography is an efficacious alternative.

Percutaneous ethanol injection [1–4], microwave coagulation therapy [5], and radiofrequency ablation [6–11] are widely performed as a percutaneous local treatment for small hepatocellular carcinomas (HCCs). Most of these treatments have been performed under real-time sonographic guidance [3, 4, 9, 10]. Sonographic targeting requires adequate visualization. However, some nodules cannot be detected clearly on conventional sonography, such as nodules in the hepatic dome, lesions deep in relation to the body surface, lesions on the liver surface, and lesions smaller than 1 cm. In addition, determination of the residual viable portion of the HCC on conventional sonography after treatment with transcatheter arterial embolization, percutaneous ethanol injection, microwave coagulation therapy, or radiofrequency ablation has also been difficult. In these cases, clinicians must mentally reconstruct a 3D model of the body from multiple 2D horizontal CT images, creating the equivalent of a sonographic image, and puncture the nodule using this conventional sonographic image for guidance. Mental reconstruction is the most important and difficult task in conventional sonography. The target site imaged by conventional sonography often differs from the site determined by CT.

MDCT offers the ability to scan large longitudinal volumes rapidly and can scan volumes over a large range within a short time with thin slices [12, 13]. MDCT images are then used to reconstruct 3D images. Multiplanar reconstructed images resemble conventional sonographic images. Using a computer system, slices are animated continuously, and the user becomes immersed in and interacts with a purely virtual, nonreal environment. We confirmed that the virtual sonographic images produced by MDCT data were equal to, and sometimes more clearly interpretable than, those of conventional sonography. In addition, we confirmed that HCC nodules depicted by virtual sonography but not by conventional sonography could be treated adequately [14]. In the present study, we evaluated the usefulness of real-time percutaneous ablation therapy under guidance using virtual sonography for HCC not visualized on sonography but visualized on CT.

Keywords: abdominal imaging, ablation, cancer, liver disease, MDCT, radiofrequency

DOI:10.2214/AJR.04.1252

Received August 6, 2004; accepted after revision March 24, 2005.

[1]All authors: Third Department of Internal Medicine, Ehime University, Sigenobutyo Sizukawa, Ehime, Japan. Address correspondence to M. Hirooka.

AJR 2006; 186:S255–S260

0361–803X/06/1865–S255

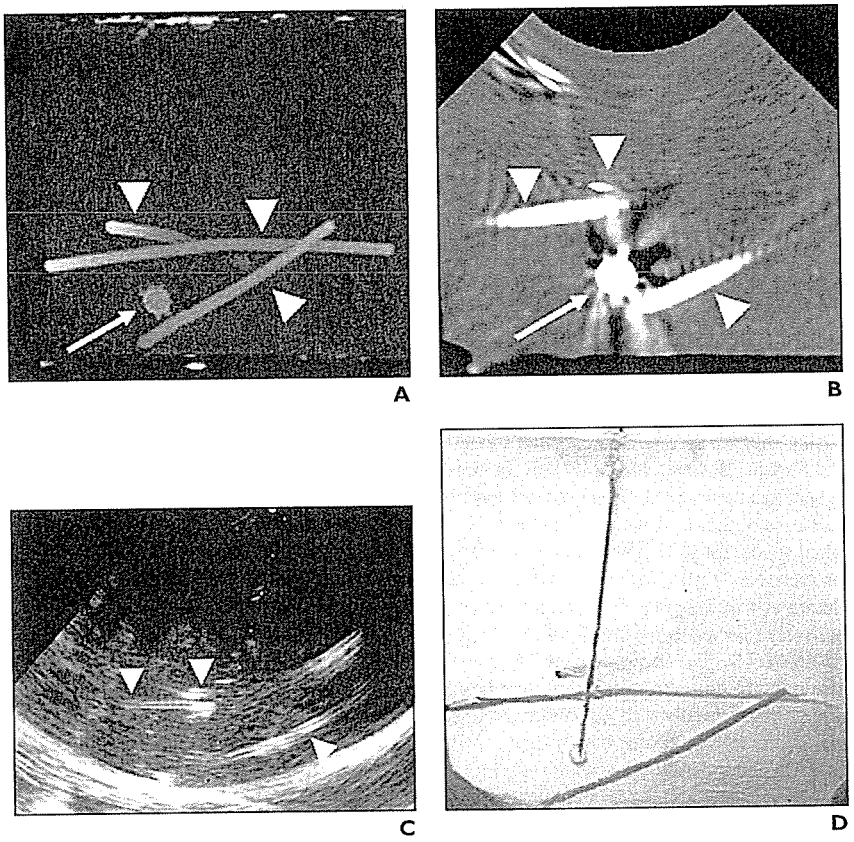

Fig. 1—Puncture procedure used for virtual sonography in gelatin gel.
A, MDCT image of gelatin gel shows small ball of contrast medium (*arrow*) and 4-French catheters (*arrowheads*) placed in phantom in such a way as to imitate tumor and vessels.
B, Virtual sonographic image is then reconstructed. Arrow indicates contrast medium; arrowheads indicate catheters.
C, Conventional sonographic image is depicted in same slice as that shown by virtual sonography. Arrowheads indicate catheters.
D, Image confirms that puncture is appropriate.

Subjects and Methods

Virtual Sonography

For synthesis of 3D images and generation of virtual sonographic images, Virtual Place Advance software (Medical Imaging Laboratory; www.milab.jp) was used. This has been described in detail in a previous communication from our laboratory [14]. In short, this system runs smoothly on a PC with Windows 2000 (Microsoft), a Xeon 2.0-GHz dual processor (Intel), 2.0 GB of random-access memory, and a graphic card with Quadro4 900XGL (NVIDIA Corp.). First, a 3D image was synthesized by CT (LightSpeed Ultra 16, GE Healthcare). The scanning parameters were a 0.625-mm collimation × 16.6 mm/sec (pitch of 1.75) table speed, 300–400 mA, 120 kV, and a 512 × 512 matrix. Then, a virtual sonographic image of the CT scan was generated. Multiplanar images were reconstructed using MDCT data, and slices were displayed in a fan shape to resemble conventional sonographic images [14].

In Vitro Experience

To evaluate the accuracy of the puncture using the virtual sonographic images, we conducted an in vitro experiment using a 16 × 9 cm piece of gelatin gel. In the gel, a target lesion modeled on the HCC nodule was made by injecting 1 mL of iomeprol contrast medium (Iomeron 300, Eisai) just before the gelatin became hard. The target lesions were placed at different depths (2.7, 3.1, 3.5, 6.4, 7.0, and 7.6 cm). A 4.0-French catheter modeled on a vessel was placed around the target (Fig. 1), and CT of the gelatin gel was then performed. A 1-cm piece of the 4.0-French catheter was placed on the surface of the gelatin gel, and a virtual sonographic image was then reconstructed through the piece. The conventional sonographic probe was placed on the site where the piece was placed, enabling sonographic images identical to the virtual sonographic images to be obtained. A 21-gauge needle was used to puncture the gelatin gel through the spot where the sonographic B-mode image was identical to the virtual sonographic image. After puncture of the gel, the distance from the target to the needle tip was measured by CT. Six target nodules were made, and each was punctured 24 times.

Clinical Experience

Patients—We examined 18 patients (14 men and 4 women; age range, 59–89 years; mean, 69.3 ± 8.07 [SD] years) with 21 HCC nodules, who had been admitted to the Third Department of Internal Medicine, Ehime University School of Medicine, Japan, between February 2004 and June 2004. All patients had liver cirrhosis. The pathogenesis of liver cirrhosis was hepatitis B in three patients and hepatitis C in 15. According to the Child-Pugh classification, 13 had class A and 5 had class B cirrhosis. The mean maximum diameter of the HCC nodules was 14.0 ± 7.81 mm (range, 5–35 mm). Of the 21 nodules, eight were in the anterior segment, eight in the posterior segment, two in the lateral segment, and three in the medial segment. HCC was diagnosed using imaging analysis, including helical dynamic CT, CT hepatic arteriography, CT during portography, and iodized oil (Lipiodol, Andre Guerbet)–enhanced CT. The patients with HCC nodules were confirmed to have elevated levels of α-fetoprotein or des-γ-carboxy-prothrombin. All HCC nodules were visualized on helical dynamic CT, CT hepatic arteriography, CT during portography, or iodized oil–enhanced CT but could not be visualized clearly on conventional sonography. Of the 21 nodules, seven had not been previously treated (initial-treatment group). The remaining 14 nodules were residual viable lesions that developed after previous treatment (additional-treatment group), with one nodule a local recurrence and the other 13 the result of an inadequate safety margin taken during initial surgery. These 14 nodules could not be distinguished from viable lesions and necrotic areas after one cycle of radiofrequency ablation.

Thirty-two patients (37 nodules; 26 men and 6 women; age range, 59–80 years; mean, 68.6 ± 5.28 years) treated between January 2002 and January 2004 without the use of virtual sonography were selected as historical control data. All these nodules were visualized on helical dynamic CT, CT hepatic arteriography, CT during portography, or iodized oil–enhanced CT but could not be visualized

clearly on conventional sonography. The patients had elevated levels of α-fetoprotein or des-γ-carboxy-prothrombin. All patients had liver cirrhosis, the pathogenesis of which was hepatitis B in six patients and hepatitis C in 26. According to the Child-Pugh classification, 24 had class A and 8 had class B cirrhosis. The mean maximum diameter of the HCC nodules was 15.7 ± 8.01 mm (range, 6–40 mm), and 16 nodules were in the anterior segment, 14 in the posterior segment, four in the lateral segment, and three in the medial segment. Of the 37 nodules, eight had not been previously treated (initial-treatment group). The remaining 29 nodules were residual viable lesions after previous treatment (additional-treatment group). Of these 29 nodules, three were local recurrences, whereas the other 26 were the result of an inadequate safety margin taken during previous surgery, and thus all required additional treatment. However, it is difficult to distinguish by only sonography those HCC nodules that were previously treated with one cycle of radiofrequency ablation from those that were not treated. The following parameters were compared between the virtual sonographic radiofrequency ablation group and the standard radiofrequency ablation group: sex, age, cause, Child-Pugh class, tumor size, session number, and local recurrence rate. Additional treatment was performed until an adequate safety margin was achieved. Patients with severe coagulation disorders (prothrombin activity < 40%, platelet count < 30,000/mL), severe cirrhosis (Child-Pugh class C), extrahepatic malignancy, or tumor thrombus in the main, left, or right portal trunk were excluded from this study. Patients were asked to provide written informed consent to enter the study, which was approved by the ethics committee of Ehime University.

Treatment—Before treatment, 15 mg of pentazocine hydrochloride and 25 mg of hydroxyzine hydrochloride were administered intramuscularly. Local anesthesia was induced by 5 mL of 1% lidocaine injected through the skin into the peritoneum along a predetermined puncture line. We inserted a 20-cm-long 17-gauge radiofrequency electrode equipped with a 2- or 3-cm-long exposed metallic tip (Cool-tip, Valleylab). First, abdominal CT was performed and the location of the cancer nodule was ascertained (Fig. 2A). Then, a virtual sonogram of the CT scan was prepared from the data of the computer (Fig. 2B). Finally, a conventional sonographic image of the virtual sonographic image was prepared. The location of the cancer nodules on the conventional sonographic image was confirmed, and they were treated by radiofrequency ablation (Fig. 2C). By measuring the distance between the HCC nodule and the vessel (hepatic or portal vein) or the surface of the liver on virtual sonography, we surmised the site of the HCC nodule on conventional sonography. If the lung was obstructing the view of the nodule, 500 mL of saline was injected into the right pleural cavity.

Estimation of Therapeutic Effect

Dynamic CT was performed between 3 and 5 days after treatment. The necrotic area of the HCC nodule and surrounding liver parenchyma was seen to be hypoattenuating during the late phases of dynamic CT. If the necrotic area depicted on posttreatment dynamic CT was larger than the viable area depicted on pretreatment dynamic CT, the therapy was considered successful [15]. If the size of the necrotic area was almost identical to that of the tumor, additional treatment was performed. Dynamic CT scans were repeated every 3 months thereafter. α-Fetoprotein and des-γ-carboxy-prothrombin assays were performed before treatment, 1 month after treatment, and every month subsequently.

Statistical Analysis

The data are expressed as mean ± SD. Statistical analysis was performed using Student's *t* test for unpaired data, contingency table analysis, and the Mann-Whitney *U* test as appropriate. A *p* value of less than 0.05 was considered to represent statistical significance.

Results

In Vitro Experience

In the in vitro experiment using gelatin gel, the puncture was performed 24 times, and six target lesions were made. The mean distance between the surface of the gelatin gel and the lesion was 5.1 ± 2.2 cm (measured by CT). The lesions were divided into two groups according to their depth from the surface of the gelatin gel: a deep group (> 5 cm deep; mean,

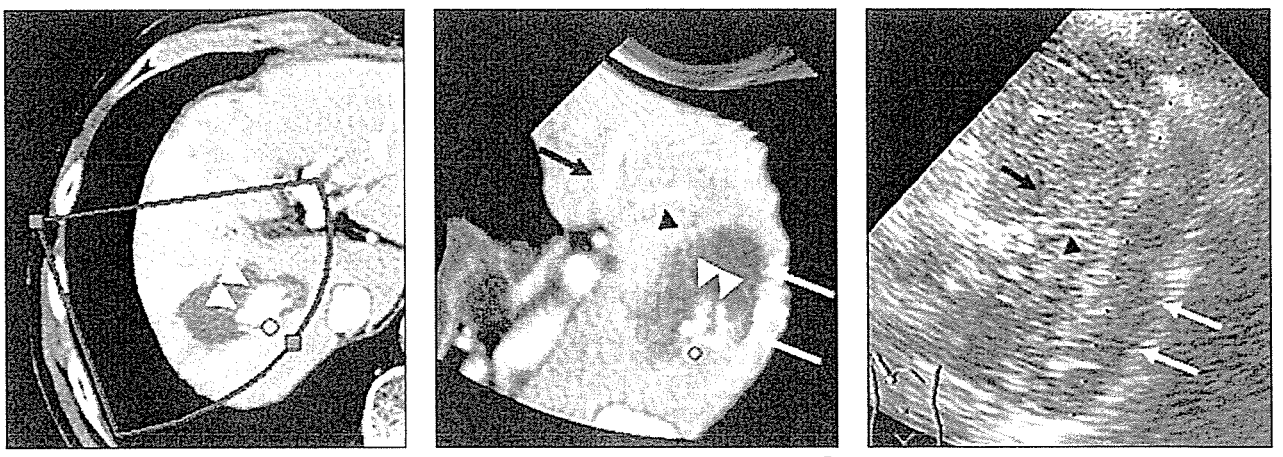

Fig. 2—72-year-old man with hepatocellular carcinoma. Construction of virtual image of hepatocellular nodule.
A, CT scan shows hepatocellular nodule (*arrowheads*).
B, Virtual sonographic image shows same nodule (*white arrowheads*).
C, Conventional sonographic image of **B**. Black arrowhead indicates cancer nodule; black and white arrows indicate previously treated areas.

7.0 ± 0.60 cm), and a surface group (< 5 cm deep; mean, 3.1 ± 0.40 cm). The mean diameter of the target lesions made by contrast medium was 1.53 ± 0.25 mm, and the mean distance between the surface of the target and the tip of the needle was 1.20 ± 0.78 mm (Fig. 1). The mean distance was 0.92 ± 0.67 mm for the surface group and 1.5 ± 0.80 mm for the deep group. Although this difference was statistically significant, punctures tended to be more accurate in the surface group ($p = 0.06$). These results confirmed that the punctures assisted by virtual sonography in the phantom model were accurate.

Clinical Experience

The shape of the liver, the vascular arrangement, and the surrounding organs indicated that the slices identified by CT and sonography were identical. We could construct virtual sonographic images identical to conventional sonographic images for all lesions. No significant difference in clinical profiles was found between virtual sonographic radiofrequency ablation and standard radiofrequency ablation in either the initial-treatment group or the additional-treatment group (Table 1). In the initial-treatment group, the mean number of virtual sonographic radiofrequency ablation treatments was significantly lower (1.3 ± 0.49) than that of standard radiofrequency ablation treatments (2.5 ± 0.76, Table 2). In the additional-treatment group, the mean number of virtual sonographic radiofrequency ablation treatments was also significantly lower (1.2 ± 0.42) than that of standard radiofrequency ablation treatments (2.0 ± 1.1, Table 2). The local recurrence rate did not differ significantly between the two initial-treatment and additional-treatment groups (Table 2). Typical cases are presented in Figures 3 and 4. The patient represented in Figure 3 had an HCC nodule that was too small to be visualized on conventional sonography in the initial treatment. This lesion was depicted on virtual sonography and was shown to be near the hepatic vein. Thus, only one puncture produced an adequate necrotic area. The patient represented in Figure 4 received additional treatment. The nodule that was treated under virtual sonographic guidance was near the necrotic area produced by previous radiofrequency ablation treatment, and its visualization was affected by pulsation of the heart. Thus, this nodule could not be detected clearly on conventional sonography but could be detected on virtual sonography. Thus, one more radiofrequency ablation treatment was performed, and after only one session an adequate necrotic area was obtained.

For radiofrequency ablation using virtual sonography, mild complications of pain and fever were noted, but no severe complications occurred. Neither α-fetoprotein nor des-γ-carboxy-prothrombin was elevated in this group, and no local recurrence took place.

TABLE 1: Characteristics of Patients Treated with Virtual Sonographic Radiofrequency Ablation and Standard Radiofrequency Ablation

Characteristic	Initial Treatment			Additional Treatment		
	Virtual Sonography ($n = 7$)	No Virtual Sonography ($n = 8$)	p	Virtual Sonography ($n = 11$)	No Virtual Sonography ($n = 24$)	p
Sex (male/female)	5/2	5/3	NS	9/2	21/3	NS
Age (yr)	66.0 ± 5.6	68.0 ± 7.3	NS	71.5 ± 8.9	68.9 ± 4.6	NS
HBV/HCV	1/6	2/6	NS	2/9	4/20	NS
Child-Pugh class (A/B)	5/2	6/2	NS	8/3	18/6	NS
Tumor size (mm)	7.4 ± 1.9	8.0 ± 2.1	NS	17.4 ± 7.6	17.8 ± 7.8	NS

Note—NS = not statistically significant, HBV = hepatitis B virus, HCV = hepatitis C virus.

TABLE 2: Comparison of Virtual Sonographic Radiofrequency Ablation with Standard Radiofrequency Ablation

Characteristic	Initial Treatment			Additional Treatment		
	Virtual Sonography ($n = 7$)	No Virtual Sonography ($n = 8$)	p	Virtual Sonography ($n = 14$)	No Virtual Sonography ($n = 29$)	p
No. of treatments	1.3 ± 0.49	2.5 ± 0.76	0.003	1.2 ± 0.42	2.0 ± 1.1	0.003
Local recurrence (%)	0	0	NS	0	3.4	NS
Complications	0	0	NS	0	1	NS

Note—NS = not statistically significant.

Discussion

The sonographic B-mode method is most suitable for detecting nodules, and thus most nonsurgical treatment for HCC has been performed under guidance by sonography [7–10]. With the progression of cirrhosis, echo signals in the liver become heterogeneous, thereby preventing identification of the target HCC nodule on conventional sonography. With conventional sonography, it has also been difficult to determine the residual viable portion of HCC after treatment with transcatheter arterial embolization, percutaneous ethanol injection, radiofrequency ablation, or combinations thereof, because of the similar appearances of necrosis and viable tumor tissue. However, sonographic targeting for these therapies requires adequate visualization of the lesions. If the lesion is not visualized on sonography but is visualized on CT, the nodule can be depicted on virtual sonography. Thus, with use of virtual sonography, HCC nodules not visualized clearly on conventional sonography can be treated.

Previously, the puncture was performed in these cases under CT guidance [16], CO_2 hepatic arteriography [17], or contrast-enhanced sonography [18–20]. Although it is possible to treat these cases under CT guidance, CT must be performed several times during therapy by conventional means. On the other hand, we performed CT only one time in patients who were treated under virtual sonographic guidance. This CT was performed before the start of therapy. In fact, several reports have described treatment performed by guided contrast-enhanced sonography [18–20]. Such imaging can reveal an enhanced residual lesion that was not visualized with the conventional sonographic B-mode method. However, identifying the safety margin may be difficult in some cases, as has been reported [21–23]. Thus, treatment guided by contrast-enhanced sonography may not serve the purpose in difficult cases. Moreover, HCC nodules on the liver surface